



OPEN

Sustainable production of 3D concrete printing using agricultural waste fibers

Sajad Garshasbi¹, Seyed Sina Mousavi², Mehdi Dehestani³✉ & Hadi Nazarpour¹

This study investigates the feasibility of using bio-waste materials as natural fibers in printability and flexural properties of 3D concrete printing (3DCP). Two sections of small- and large-scale experimental programs were conducted using natural fibers derived from bio-waste of date palm, cob skin, banana, pineapple leaf, and coconut fibers with different volume fractions of 0.1%, 0.15%, 0.2%, and 0.25%. Different tests were conducted in the small-scale program, including flowability, extrudability, buildability, open time, compressive strength, tensile strength, and flexural strength. After achieving an optimum percentage of natural fibers, 3DCP beams were tested under flexural loading. The optimum fiber volume fraction of 0.2% was determined through an experimental program evaluating fresh and mechanical properties, balancing enhanced strength with printability. Findings showed that using recycled bio-fibers enhanced the strength of both cast and 3DCP samples. Incorporating 0.2% by volume of date palm, cob skin, banana, pineapple leaf, or coconut fibers individually led to average increases of 26% in compressive strength, 40% in tensile strength, and 20% in flexural strength, and an average decrease of 10% in flowability and 8% in extrudability compared to mixtures devoid of fibers. Furthermore, the fibers contributed to maintaining the shape and stability of the printed filaments—nonetheless, higher fiber content impaired flowability and extrudability. Future research could explore hybrid fiber systems, advanced additives, and long-term durability to further enhance the sustainability and scalability of fiber-reinforced 3DCP.

Keywords 3D concrete printing, Natural fibers, Plant fibers, Sustainability, Bio-waste

3D concrete printing has the potential to revolutionize the construction industry¹. This method uses layer-by-layer extrusion of concrete without the need for traditional formwork, reducing costs, time, and resource consumption^{3,4}. Furthermore, by providing a greater range of shapes, this invention would liberate the architectural gesture⁵. Research in the field of 3D concrete printing (3DCP) has significantly expanded over recent years^{6–9}, demonstrating how the financial and environmental aspects of large-scale 3DP concrete constructions still require optimization despite substantially lower labor and formwork costs, printable materials are not cheap when compared to ordinary concrete.

The construction sector is responsible for a significant portion of global greenhouse gas emissions (GHGs) and solid waste generation¹⁰. Therefore, it is essential to find sustainable methods and materials to mitigate the adverse environmental and societal impacts of this industry. To this end, research has been conducted on developing new binders with low clinker content^{11,12}, geopolymers concretes^{13,14}, and aggregates recycled from construction waste, slags, and biowastes. In recent years, cement-based composites have been increasingly reinforced with various types of fibers, including steel, glass, carbon, and organic synthetic fibers, as is well known. However, the use of these fiber types presents certain limitations¹¹. Plant fibers are widely found in nature. These fibers are low-cost, renewable, and effectively strengthen cement-based composites. Incorporating plant fiber significantly enhances the flexural strength of cement-based composites¹² and prevents the formation of microcracks in the matrix⁸. At the same time, these fibers are also gradually used for the 3D printing of composites and geopolymers (3DPGs)⁹. The primary constraint on 3D concrete printing is the choice of a printable concrete mixture. A printed mix's primary difficulty is balancing necessary flow and stability, two opposing goals^{10,11}.

Previous studies have been done with recycled natural fibers (sometimes called plant fibers) in various types of concrete^{12–14}. Regarding 3D concrete printing, Kornienko and Łach¹⁵ discussed the effect of short and

¹Graduate Student, Faculty of Civil Engineering, Babol Noshirvani University of Technology, Postal Box: 484, Babol 47148-71167, Iran. ²Post-Doctoral Fellow, Faculty of Civil Engineering, Babol Noshirvani University of Technology, Postal Box: 484, Babol 47148-71167, Iran. ³Faculty of Civil Engineering, Babol Noshirvani University of Technology, Postal Box: 484, Babol 47148-71167, Iran. ✉email: dehestani@nit.ac.ir

long fibers in mechanical properties of geopolymer composites, especially those based on fly ash. According to the study, fiber reinforcement enhances the mechanical characteristics of 3D-printed geopolymers, offering them a viable substitute for conventional concrete. Panda et al. investigated how short glass fibers affected the 3DPC material's mechanical performance. The addition of glass fibers improved the flexural and tensile strength of the printed specimens¹⁶. Nematollahi et al. examined the impact of PP fibers in properties of 3D-printed fiber-reinforced geopolymer mortars, both at the fresh and hardened stages¹⁷. Additionally, Nematollahi and colleagues examined the effects of three different plastic fibers (PVA, PP, and PBO fibers) on the inter-layer bond and flexural strengths of extrusion-based 3D printed geopolymer¹⁸. Due to the ever-growing environmental concerns, researchers have substituted plant fibers for steel or synthetic fibers in composite materials like concrete, mortar, and cement paste^{19–21}. Coconut, sisal, jute, pineapple leaf, kenaf bast, bamboo, palm, banana, hemp, flax, cotton, and sugarcane fibers are some examples of these natural fibers. Natural fibers are inexpensive and widely accessible in many nations. When eco-friendly natural fibers replace synthetic fibers, significant greenhouse gasses can be eliminated. Thus, incineration and landfill operations, often used to process synthetic composite waste, should be avoided during the end-of-life (EOL) phase due to high CO₂ emissions in the air and groundwater²². In the last few years, studies have been conducted on using natural and plant fibers in the application of 3D concrete printing. Natural fibers are biodegradable and have a lower environmental impact compared to synthetic fibers. Also, these fibers can enhance the mechanical properties of cementitious composites, such as flexural strength and impact resistance. Natural fibers also improve ductility and energy absorption, which can delay crack propagation and prevent structural failures. In 2020, Luhar et al.⁹ provided a comprehensive review of natural fibers' current performance and benefits in conventional concrete construction. The integration of natural fibers into 3D printable materials requires careful consideration of the mixture design to ensure good printability, including factors like extrudability and buildability. Luhar et al. also highlighted the potential of natural fibers to overcome consistency and shrinkage problems in 3DPC. Integrating 3DCP with environmentally friendly materials like recycled aggregate concrete and plant fibers allows for preserving structural integrity while reducing environmental effects^{23–25}. Yu et al.²⁶ examined the combination of plant fibers and recycled aggregate concrete (RAC) using 3D printing. Studies indicate that using fibers can mitigate RAC's adverse impacts on performance in 3D printing, especially in terms of tensile and flexural strength. These results suggest that adding plant fibers will optimize mechanical qualities. Nowadays, cellulose-ether derivatives (CEs), such as viscosity-modifying agents (VMAs) or viscosity-enhancing additives, are the primary application of supplementary cementitious materials (SCMs) in 3DCP^{27–30}. Nonetheless, very few studies have been conducted on the efficacy of SCMs for 3DCP.

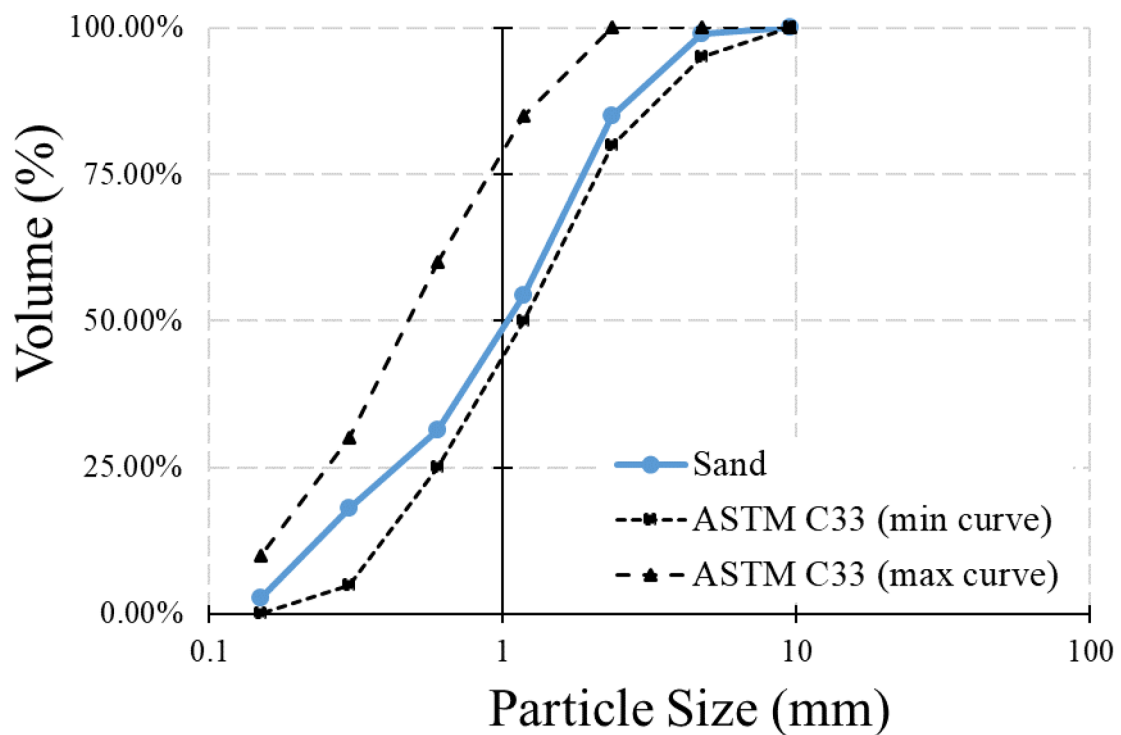
The incorporation of natural fibers derived from bio-waste, such as date palm, cob skin, banana, pineapple leaf, and coconut fibers, into 3D concrete printing (3DCP) offers significant potential for sustainable construction applications. These fibers, sourced from abundant agricultural waste, provide an environmentally friendly alternative to synthetic fibers, reducing the carbon footprint and waste associated with construction materials⁹. For instance, coconut fiber has been successfully used in precast concrete elements and non-structural components, enhancing tensile and flexural strengths while maintaining cost-effectiveness¹⁹. By leveraging these fibers in 3DCP, the construction industry can achieve greater sustainability, particularly in developing countries where bio-waste is readily available, thereby reducing reliance on energy-intensive materials and promoting circular economy principles³¹. This study explores these fibers' potential to enhance the mechanical and rheological properties of 3D-printed concrete, paving the way for scalable, eco-friendly construction solutions.

Recent literature has made significant strides in researching ways to improve the sustainability of 3D printable concrete, particularly by exploring the use of waste materials. However, there are still notable research gaps, and further experimental work is needed to advance this area^{32–36}. Moreover, some studies concentrated on using fibers in 3D printable concrete mixtures^{37–39}, whereas minimal specific studies comprehensively worked on recycled fibers-reinforced 3DCP⁴⁰. Accordingly, this study investigates the effect of different natural fibers derived from bio-waste on the rheological and mechanical properties of 3D concrete mixtures. Various percentages of bio-waste such as palm fiber, cob skin, banana fiber, pineapple leaf fiber (PALF), and coconut fiber (Coir) for testing fresh and hardened concrete have been used. Hence, the main goals of this research are as follows:

- To characterize the effect of natural fibers derived from bio-waste on the fresh and printability properties of 3D printable concrete.
- To evaluate the influence of natural fibers derived from bio-waste on the mechanical properties of 3D printable mortars.
- To determine the optimum mix design of 3D printable mortar incorporating various natural fibers, including the type and volume fraction.
- To assess the structural performance of 3D-printed beams reinforced with natural fibers compared to cast specimens.

To accomplish these goals, the current experimental program is divided into two distinct sections. The first section involves conducting small-scale tests to assess the impact of fibers on the flowability, printability, buildability, and mechanical performance of mortars. Once the optimal dosage of natural fibers is determined, the resulting mix design is used to create printed beams, which are then compared with cast specimens. Additionally, this study explores the hardened properties of 3D-printed samples from multiple directions.

Chemical composition	OPC	Bentonite	GGBS	LP
SiO ₂	21.25	65.5	37.5	0.015
Al ₂ O ₃	5.25	16.95	10.65	0.074
Fe ₂ O ₃	3.86	3.5	0.3	0.24
CaO	63.96	1.34	34.65	57.84
MgO	1.13	3.15	8.11	0.122
Na ₂ O	0.34	1.15	0.65	0.103
K ₂ O	0.58	0.51	1.3	0.036
TiO ₂	-	0.14	4.38	0.012
MnO	-	0.13	2.45	-
P ₂ O ₅	-	0.03	-	-
SO ₃	2.2	-	-	-
LOI	1.4	7.6	-	41.55

Table 1. Chemical composition of different Raw materials (mass %).**Fig. 1.** Particle size distribution for sand.

Materials and methods

Material design

The binder for the printable concrete mix used in this study consists of Ordinary Portland cement (OPC) and bentonite. Also, limestone powder (LP) and ground granulated blast-furnace slag (GGBS) were used as powder materials in mixtures. Table 1 shows the chemical composition of the raw materials. According to ASTM C136⁴¹, sieve analysis was used to determine the particle size distribution of the sands. Figure 1 shows the particle size distribution of sand. The sand was passed through an 8-inch sieve (maximum size 2.36 mm) to have a high print resolution. A liquid superplasticizer (SP) based on polycarboxylate ether (PCE) was also used to modify the mix's workability. Further, the use of natural fibers was also investigated, and among them, date palm (DPF), cob skin (CF), banana (BF), pineapple leaf (PALF), and coconut fibers (Coir) were tested. All the fibers were cut to a specific length and width (Fig. 2). The fiber lengths, as shown in Table 2, range from 0.8 mm (cob skin) to 12 mm (coconut), with date palm, banana, and pineapple leaf fibers at 12 mm, 10 mm, and 10 mm, respectively. These lengths were chosen to exceed the estimated critical fiber length (approximately 2–5 mm) for effective stress transfer in the cementitious matrix, as supported by prior studies^{19,20}. The lignocellulosic fibers were washed, dried, and cut to remove impurities but were not subjected to alkaline treatment to maintain their natural state and minimize processing costs. This approach aligns with sustainable 3DCP goals, though untreated fibers may



Fig. 2. Natural fibers used for the preliminary 3DP mixtures: **a)** date palm fibers (DPF); cob skin fibers (CF); banana fibers (BF); pineapple leaf fibers (PALF); coconut fibers (Coir).

Natural fibers	Average diameter (mm)	Average length (mm)	Density (g/cm ³)	Tensile strength (MPa)	Water Absorption (%)	Cellulose Content (%)	References
Date palm	0.5	12	0.7–1.55	58–203	20–30	40–50	80
Cob skin	1.2	0.8	1.1–1.58	15–45	10–20	30–40	81
Banana	1.0	10	1.35	529–914	10–15	60–65	82
Pineapple	1.0	10	0.8–1.6	170–1627	12–20	70–80	83
coconut	0.3	12	1.2–1.5	175	10–15	30–40	84

Table 2. Mechanical properties of natural fibers in this study.

exhibit higher hydrophilicity, potentially affecting long-term durability^{13,14}. The size of the fiber, particularly its length and diameter, influences the rate of water absorption due to increased surface area, as reported in prior studies^{20,42}. The amount of water absorbed increases with fiber length. Fibers' morphology and chemical makeup were examined using a scanning electron microscope (SEM). The SEM image of the fibers' surface is shown in Fig. 3. Table 2 shows the properties of selected natural fibers. The tensile strength, density, water absorption and cellulose content values of the fibers were obtained from the previous literature^{43,44}.

The natural fibers used in this study were processed to remove impurities while preserving their natural properties to align with the sustainability goals of the study. The fibers were sourced from agricultural waste and subjected to a cleaning process involving washing with distilled water to remove dirt, debris, and organic residues, followed by air-drying at 25 °C for 48 h. The fibers were then manually cut to the specified lengths (Table 2) to ensure uniformity. Alkaline treatment, commonly used to enhance fiber-matrix adhesion by reducing hydrophilicity, was intentionally avoided to minimize processing costs and environmental impact, as chemical treatments can introduce additional energy consumption and waste^{45,46}. However, the absence of chemical treatment may increase the fibers biodegradability and water absorption, potentially affecting the long-term durability of the composites⁴⁷. The untreated fibers lignocellulosic structure, rich in cellulose, hemicellulose, and lignin, contributes to their biodegradability, making them suitable for applications where environmental degradation is acceptable, such as temporary structures or non-critical elements. Future studies could explore minimal chemical treatments to balance durability and sustainability.

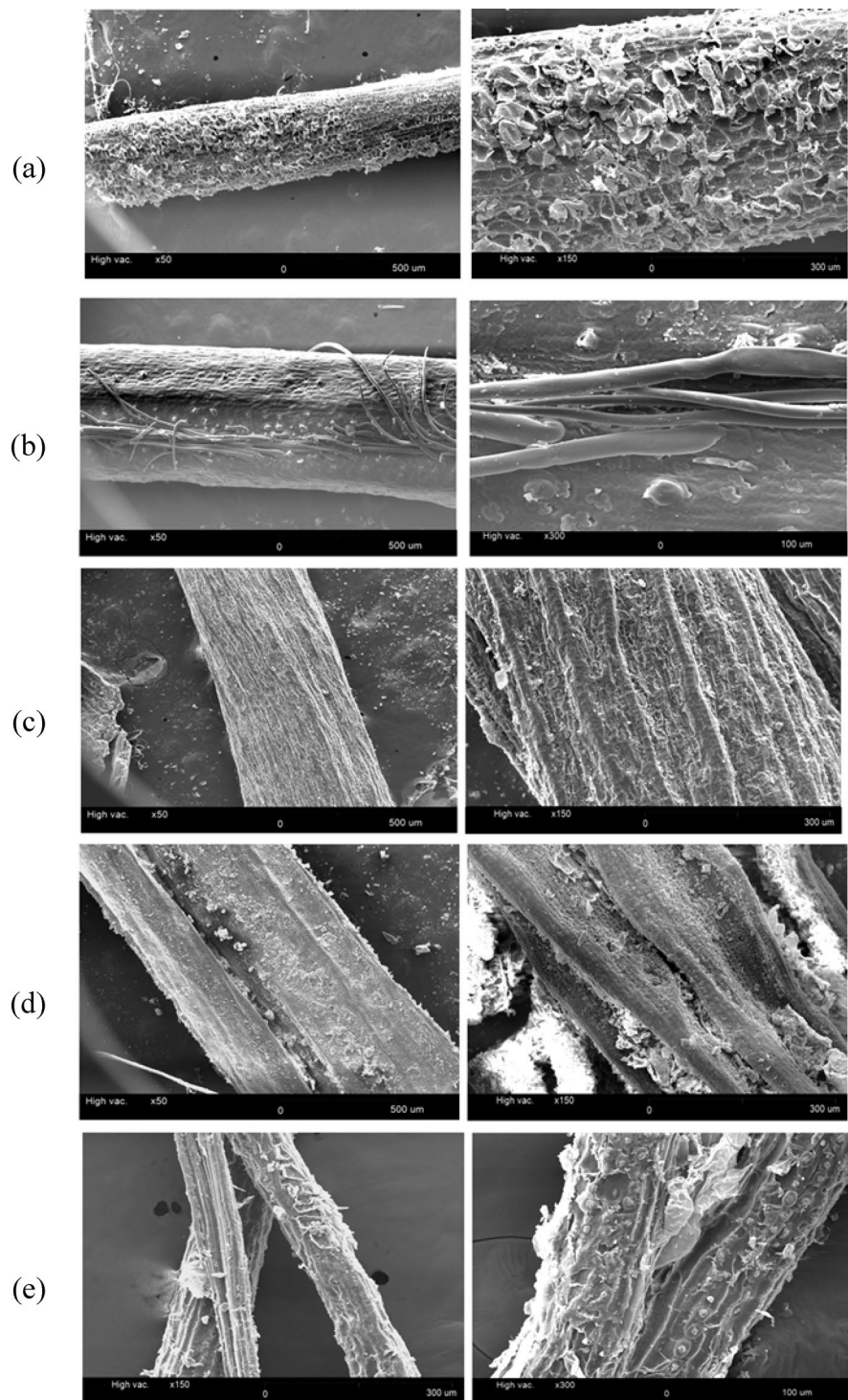


Fig. 3. SEM images of bio-waste fibers: (a) date palm fiber (DPF); (b) cob skin fiber (CF); (c) banana fiber (BF); (d) pineapple leaf fiber (PALF); (e) coconut fiber (Coir).

Mix Preparation

The 3D printable concrete mixture must meet the requirements of fresh and hardened concrete. These requirements include flowability, extrudability, and buildability of mixtures. The compressive and flexural strengths of the printed and cast specimens are the essential characteristics of the hardened concrete. To design a suitable 3DP mix, five types of natural fibers in four different volume percentages were used. In total, mixtures were prepared with $W/P = 0.5$ and $S/P = 1.2$ ratio. In the present study, 21 mixtures with different proportions and amounts of fibers were made to improve the characteristics of fresh and hardened concrete and to select the most optimal printable mortar and optimum percentage of fiber by comparing the mixes. The mix proportions

of the mixtures being studied are summarized in Table 3. According to the standard ASTM C305⁴⁸, water was first poured into the container, and binders and powders were added. Start the mixer and mix slowly at the rate of 140 ± 5 r/min for 30 s. Then, the mixer is turned off for 30 s, and after that, sand is added to the mixture for 30 s; the mixer starts mixing the ingredients at a medium speed (285 ± 10 r/min). After that, the weighed fibers were added to the mixer. The fibers were added as volume fractions. Then, the superplasticizer was added to the mixing water to reduce the ratio of water to the binder and thus increase its efficiency and strength. Superplasticizer was added to the mixtures at a rate of 1% based on the weight of the binder. Finish by mixing for 60 s at medium speed. This study determined fiber dosage by the need for printability and strength. Higher fiber dosages result in difficulty during extrusion.

Experimental tests

Given the significant differences between 3D-printed concrete construction and traditional construction, it is imperative to comprehend the fresh properties of the 3DPC mixture and its assessment techniques. As acknowledged in this section, the material parameters are flowability, extrudability, buildability, open time, and rest time. In addition, the characteristics of hardened concrete are essential to determine the suitable mortar for printing. The primary purpose of 3DPC structures is to achieve high compressive strength, flexural strength, and tensile strength for cast and printed mortars.

Flowability

The flowability of concrete mixtures is a vital parameter for their printable performance. Generally, it describes a material's capacity to move and hold its shape under pressure without losing its original characteristics. Rheological properties and flow behavior can vary significantly across different materials and conditions. This variability is influenced by factors such as particle interactions, temperature, and the presence of additives, which can lead to diverse flow behaviors. The determination of the flow value of mixtures was conducted through the execution of the flow table test in accordance with the ASTM C1437⁴⁹ standards. This flow table test, distinct from the slump test (ASTM C143), measures the spread diameter of mortar after 25 jolts, providing insight into its rheological behavior under dynamic conditions. To test the flow table, the mortar was poured into a conical mold and compacted. Then, the mold was pulled out, and the table was hit 25 times for 15 s. Then, the spread diameter was measured on two sides (D1 and D2), and its average was calculated as the flow value of each mixture. The particle size of the concrete ingredient is a major determinant of its rheology and fluidity in the fresh state.

Extrudability

Another important parameter for 3DPC is extrudability. The ability of a 3D printable material to be continuously compressed from a nozzle while preserving the necessary layer quality and dimensional accuracy is referred to as extrudability. The layer quality means the printed layer should be free from defects such as voids and discontinuation. There are no actual norms available for extrudability testing. The researchers have determined

Mix ID	OPC	Sand	Bentonite	GGBFS	LP	Water	Fibers (%)
F0-0	490	840	70	105	35	350	0
F1-0.1DPF	490	840	70	105	35	350	0.10
F2-0.1CF	490	840	70	105	35	350	0.10
F3-0.1BF	490	840	70	105	35	350	0.10
F4-0.1PALF	490	840	70	105	35	350	0.10
F5-0.1Coir	490	840	70	105	35	350	0.10
F6-0.25DPF	490	840	70	105	35	350	0.25
F7-0.25CF	490	840	70	105	35	350	0.25
F8-0.25BF	490	840	70	105	35	350	0.25
F9-0.25PALF	490	840	70	105	35	350	0.25
F10-0.25Coir	490	840	70	105	35	350	0.25
F11-0.15DPF	490	840	70	105	35	350	0.15
F12-0.15CF	490	840	70	105	35	350	0.15
F13-0.15BF	490	840	70	105	35	350	0.15
F14-0.15PALF	490	840	70	105	35	350	0.15
F15-0.15Coir	490	840	70	105	35	350	0.15
F16-0.2DPF	490	840	70	105	35	350	0.2
F17-0.2CF	490	840	70	105	35	350	0.2
F18-0.2BF	490	840	70	105	35	350	0.2
F19-0.2PALF	490	840	70	105	35	350	0.2
F20-0.2Coir	490	840	70	105	35	350	0.2

Table 3. Mix proportions of the 3D printable mortars tested in the present study (kg/m^3).

the maximum printing distance at which the filament can be extruded without experiencing any fracture, blockage, segregation, or bleeding by using the visual inspection method for extruded layers or filament^{50,51}. This research evaluated the extrudability with 35 mm wide filaments (printed from a 35 mm nozzle). The extrudability of materials can be well-checked and measured using ram extruders. Therefore, an extrusion device that acts as a piston-cylinder has been used to compare the length of time that the mortar can be extruded from a nozzle without any blockage or signs of cracking and separation. To conduct the test, the material was poured into the tube, and a constant force was applied to the piston by the universal jack to print a mortar line.

To perform the extrudability test, the mortar was poured into a cylindrical tube with a diameter of 100 mm and a height of 200 mm, and with the pressure of the piston, the extruded mortar was printed through a 30 mm nozzle. Also, before the beginning of the printing operation, the inside of the pipe is lubricated with oil to further reduce the effect of pipe friction. A qualitative test was used to check the extrudability of the mixtures so that there was no blockage or breakage in an extruded strand. The extrudability test was performed 5 min after mixing with constant piston pressure by universal jack to make a correct comparison between the mixtures in terms of extrudability.

Buildability

Another basic parameter used to evaluate the printable performance of cement-based materials is the buildability and shape stability of printed mortars in several layers. The buildability of fresh mortar depends on its thixotropy and viscosity properties. Buildability is defined as the ability of an extruded layer to maintain its shape under the weight of successive upper layers. Visual inspection, counting the number of layers, and measuring the deformation of layers are used to assess buildability. To check the buildability and maintain the shape of the fresh mortar immediately after construction, it is poured into a cylindrical mold with a height of 50 mm ($H_0 = 50$ mm), and steel sheets with an approximate weight of 95 gr are placed on the mortar. After demolding, plates were put on top of the fresh samples. The main advantage of this test is that there is no need to print concrete layers, which leads to time savings in the mix design phase. Finally, the number of weights and the sample's final height before collapse (H_1) are determined. Plastic collapse, stability failure, or both can be blamed for printing failure brought on by inadequate buildability. Plastic collapse is the failure of a material as a result of the compressive load (σ_C) being greater than the material's compressive strength (σ_M), such that $\sigma_C = \rho gh(t)$, where g is the gravitational acceleration constant, ρ is the material's density, and $h(t)$ is the printed component's height as it varies over time⁵². In contrast, stability failure arises from the local or global instability of the printed structure, leading to buckling and, ultimately, the collapse and failure of the structure⁵³.

Open time

The duration of time that the material flows easily through the nozzle without becoming clogged or blocked is known as the open time. A cementitious material's setting time, typically measured with a Vicat apparatus, is correlated with its open time. Nevertheless, the purpose of this equipment is to measure the initial and final setting times, which are not very useful for characterizing how the workability of fresh concrete changes over time. To achieve good printability, the printable mix must have an open time longer than required for material extrusion. In this study, the duration during which fresh concrete's workability was sufficient to preserve its extrudability was defined as the open time. To perform this test, the extrusion system extruded a layer of mortars at 5, 10, 15, 20, 30, 45, and 60 min, and the length and width of the extruded mortars were compared to evaluate the open time.

Mechanical strength

Suitable materials for 3D printing should have the desired mechanical strength in addition to the characteristics of fresh mortar. Due to this, the main target of 3DPC structures is to attain high strength in compression, flexural strength, and tensile strength in all directions. Compressive strength is regarded as the conventional concrete quality criterion. The compressive strength was determined using 50 × 50 × 50 mm cubes according to the standard ASTM C109⁵⁴. For printed concrete, six cubes of the three-layer printed element with a length of 30 cm, a width, and a height of 5 cm were separated and tested in three different loading directions (X, Y, and Z). The printing and casting specimens were placed in water, and the CTM machine performed the 1, 7, and 28-day compressive tests with a loading rate of 900 N/s. Two samples were taken for each set, and the 28-day compressive strength of the cast and printed specimens were compared.

Also, the printed element with two layers was saw-cut into 40 × 40 × 160 mm prisms to evaluate the flexural strength under three-point bending in two different loading directions (Y and Z) after curing at 28 days. These prisms were obtained by saw-cutting larger printed elements (40 mm high, 300 mm long, two layers) using a water-cooled diamond blade saw after 28 days of curing, ensuring precise dimensions and preserving interlayer bonding, as per established 3DCP testing protocols⁷. To compare the mold-cast flexural strength, six standard specimens were cast and tested in bending at 1 and 28 days. The test procedure and the loading rate were in accordance with ASTM C348¹. This three-point bending test, conducted per ASTM C348, evaluated the flexural strength of prisms in the Y and Z directions. Additionally, a four-point bending test was performed on larger beams (10 × 10 × 50 cm) to assess structural performance, following ASTM C1609, as detailed in Sect. “**Pull-out Bond strength**”. Considering that 3DPC builds the entire object layer by layer, bond strength is regarded as one of the most crucial factors in guaranteeing structural stability. To understand the strength between the printed layers a direct tensile test has been used. For this purpose, each casting sample was poured into a brackets mold and tested under a direct tensile test in 28 days. A schematic representation of saw-cut specimens and different printing directions is shown in Fig. 4.

To evaluate the interfacial bond strength between natural fibers and the 3D printed concrete matrix, a briquette test was performed, adapted from methods described in previous studies^{55–58}. The briquette specimens

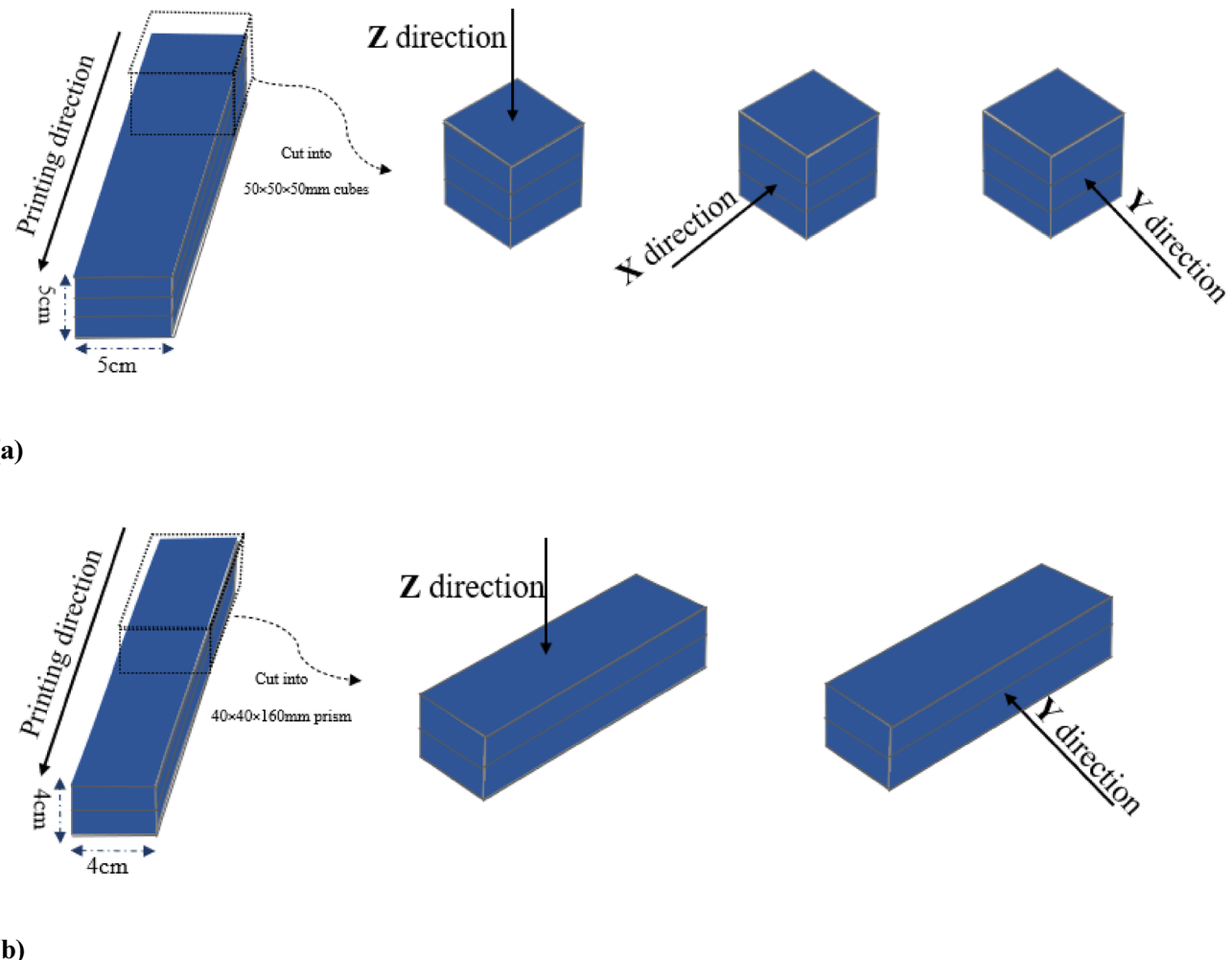


Fig. 4. Illustration of cutting and direction of 3DCP specimen for mechanical test: (a) Compressive specimens; (b) flexural specimens.

were prepared by first filling half of the mold with the mortar mixture. Ten natural fibers, each with a length of 20 mm, were carefully embedded into the fresh mortar such that 10 mm of each fiber was embedded, and the remaining 10 mm protruded from the mortar surface. This embedment length was selected to exceed the critical fiber length, ensuring effective stress transfer within the cementitious matrix, as supported by previous research^{58,59}. The specimens were demolded after 24 h and cured in a water tank. The pull-out tests were performed using a MTM testing machine with a loading rate of 0.5 mm/min, ensuring gradual stress application to accurately capture the bond strength (Fig. 5). The decision to use ten fibers per specimen, as opposed to four steel fibers used in similar studies with synthetic fibers⁵⁷, was driven by the unique properties of natural fibers. Natural fibers, such as those derived from agricultural waste, exhibit greater variability in diameter, surface roughness, and mechanical properties compared to steel fibers⁶⁰. By increasing the number of fibers to ten, the experimental variability was minimized, enhancing the statistical reliability of the bond strength measurements. This approach aligns with recommendations for testing natural fiber-reinforced composites, where higher sample sizes are often employed to account for material heterogeneity⁶¹. For each fiber type, three briquette specimens were tested to ensure repeatability. When evaluating the interfacial bond performance of a fiber-matrix interface, the bond strength is a crucial metric. This is how it is determined, per various relevant studies^{55,57,62–64}:

$$\tau = \frac{P}{n\pi dl} \quad (\text{in MPa}) \quad (1)$$

where τ is the bond strength, P is the peak load during a pull-out test, d (mm) is the diameter of the natural fiber, l (mm) is the fiber embedment length in the pull-out part, and n is the number of fibers fixed in a specimen.

3D printing test setup

The cartesian-type 3D printer having a working space of 1 m length, 0.8 m width, and 0.8 m height was used in this study. The printer's X, Y, and Z directional movement was monitored using Pronterface (Printrun) software V2.0.1 (<https://github.com/kliment/Printrun>), an open-source tool that facilitates precise control of the printer's

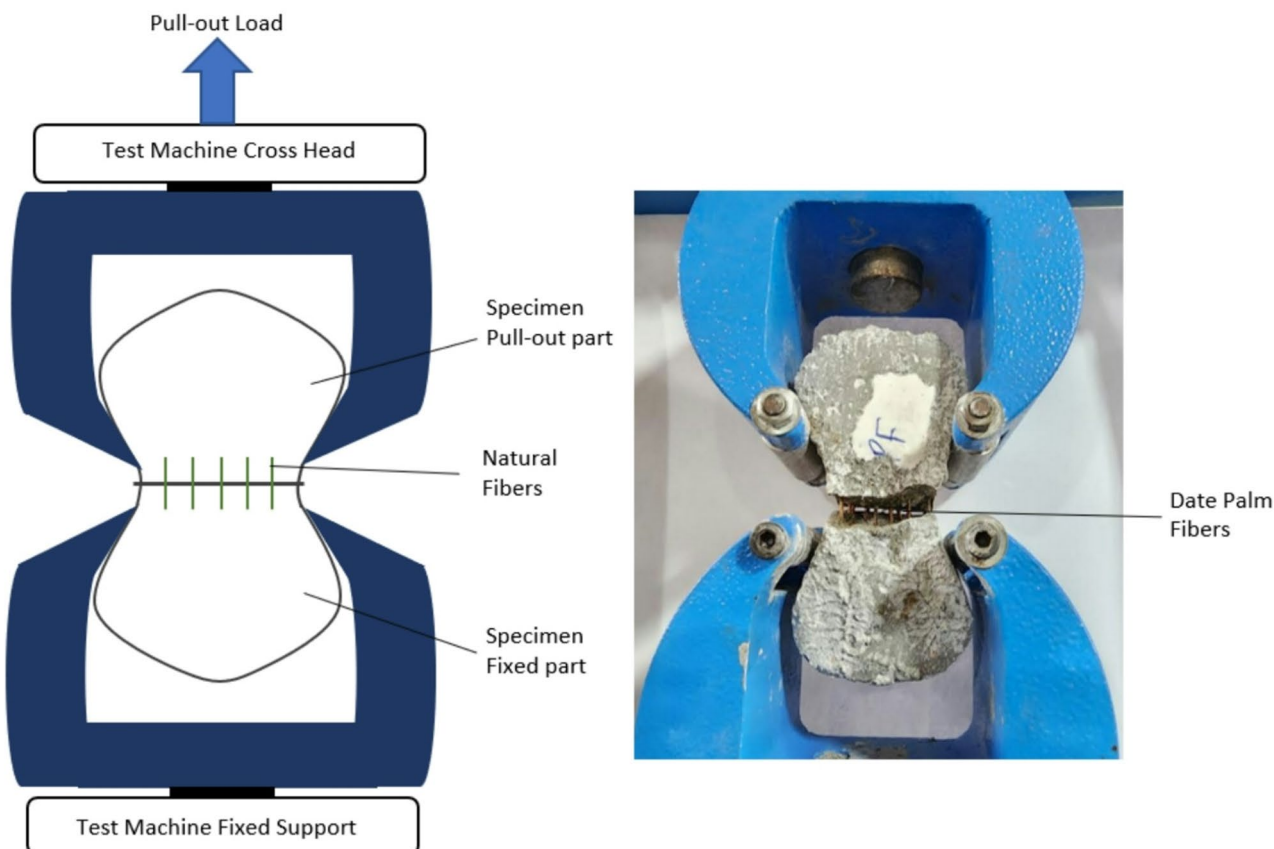


Fig. 5. The test setup used in pull-out tests and broken sample.

stepper motors and real-time monitoring of the printing process. Pronterface was configured to operate at a movement speed of 2000 mm/min in the X and Y directions and 200 mm/min in the Z direction, ensuring consistent layer deposition and alignment. A conical tank with a tube 20 cm in length and 8 cm in diameter is placed on the printer as an extruder, which includes a spiral inside the tube, which is driven by a stepper motor with a constant speed of 200 mm/s to direct the mortar to the printer nozzle. A nozzle with a circular cross-section diameter of 40 mm was used. The 3D printer in this study and the extruder head are shown in Fig. 6a. The materials were added to the mixer before the specimens were printed, and once thoroughly mixed, the mortar was ready for 3D printing. Then, the mortar was poured into the material container on the 3D printer. According to the 3D model given to the Simplify3D software V4.1.2 (<https://www.simplify3d.com>), the printing path was transferred to the printer, and samples with different lengths and heights were printed in several layers (Fig. 6b). Simplify3D allowed for precise adjustment of printing parameters, including layer height, nozzle diameter, and extrusion rate, ensuring dimensional accuracy and print quality. The X-direction is the main path of 3D printing. The movement speed of the printer was 2000 mm/min in the X and Y directions and 200 mm/min in the Z direction. The height distance of the nozzle from each layer and the printing time of each layer depends on the dimensions of the printed element. To make compression samples, mortar with a width of 5 cm was printed in three layers, and for bending samples, a width of 4 cm was considered in two layers. However, in the end, by determining the optimal percentage of fiber, beams with a length of 50 cm and width and height of 10 cm were printed in 4 layers with a thickness of 2.5 cm in each layer.

Results and discussion

Flowability

Figure 7 shows the flow table test for some of the investigated mixtures. Flow table tests were performed for the mixtures immediately after fabrication. The flowability of mortars decreases with time. The results of the flow table test and spread diameter of mixtures are depicted in Fig. 7. Spread diameter of 196.25 mm was considered for the reference mortar (F0-0%) without fiber. No additional water was used for the mixture to precisely monitor the workability reduction in mixtures. Mineral admixtures are small in particle size and have a high specific surface area. The inclusion of a granulated blast-furnace slag (GGBFS) helps increase flowability. The addition of bentonite clay and limestone powder reduces the flow of the mix and increases the water demand⁶⁵. Also, the inclusion of fiber content has an adverse effect on the flowability of the mix⁶⁶. As can be seen, adding fibers at a content of 0.1% reduces the flowability of the mixture by 8%. This amount reaches 10% for a fiber content of 0.25%. However, due to the small size of the fibers and the low fiber content in the mixture, it does not cause

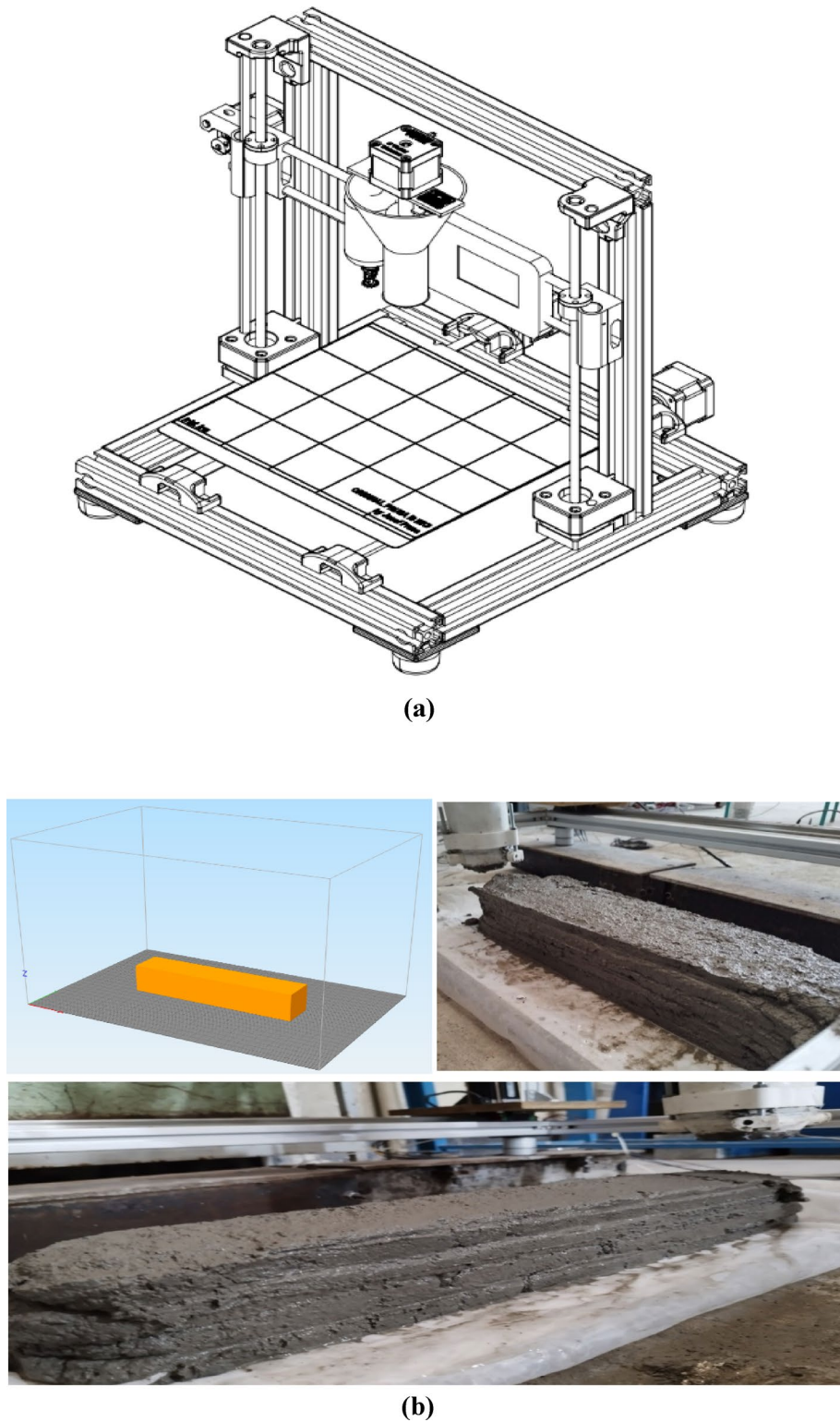


Fig. 6. Overall representation of 3D printing test: (a) 3D printer machine; (b) 3D model and printed mortar.

problems with flowability, and mortars containing fibers are suitable for 3D printing. Adding natural fibers to 3D concrete printable mixtures reduces slump and flowability due to increased internal friction and resistance to flow, as well as the hindrance of cement matrix deformation⁹. On the other hand, the type of natural fibers used can affect the flowability of the mixture. Adding coconut fibers (coir) to the mixture will have the most significant effect on reducing flowability. This can be considered due to the lower weight of coconut fibers and its longer bond length in the mixture. In contrast, DPF, BF, and CF will have the least amount of water absorption and have

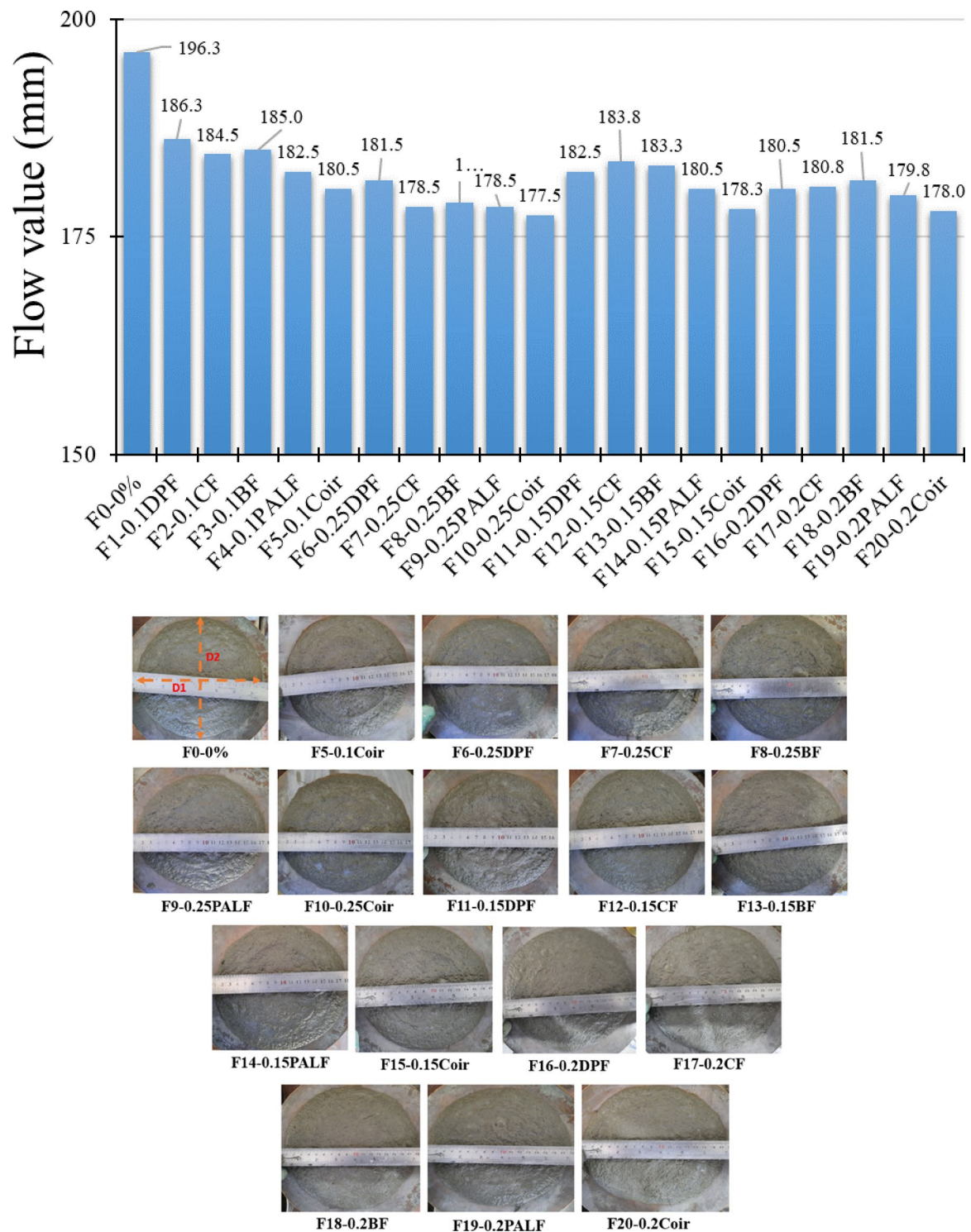


Fig. 7. Results of flow value of mixtures.

the most minor effect in mortar slump. Among them, date palm fiber has the largest flow value due to its small diameter compared to other fibers. Obviously, increasing the content of fibers from 0.1 to 0.25% decreases the spread diameter, although slightly. But this amount is not such that it disturbs the workability of the mixture. These findings align with prior research indicating that natural fibers increase internal friction in cementitious mixtures, reducing flowability^{9,67}. However, our study demonstrates that low fiber contents (0.1–0.2%) maintain sufficient workability for 3DCP, unlike higher fiber dosages reported by Chen et al. (2019)²⁷, which significantly impaired extrusion. This suggests that bio-waste fibers like date palm and coconut offer a sustainable alternative to synthetic fibers while preserving printability.

Extrudability

Figure 8. shows the different lengths of mortars extruded by the extrusion setup. The goal was to continuously print mortar with a length of 350 mm in a period of 180 s. The mixtures were compared regarding the length of time the cement paste could be extruded from a nozzle without any clogging or signs of cracking. From our test results, all fresh mixtures were continuously extruded without disruption, segregation, and blockage, indicating acceptable extrudability. The extrudability of the 3D printable mixture is mainly dependent upon factors including water-to-binder (W/B) ratio, sand-to-binder (S/B) ratio, rheological properties of the mix, load speed of the piston in the ram extruder, and size of the nozzle. Also, the size of aggregate particles and the type and length of fibers can affect the extrudability of the mixture⁶⁸. Most researchers discovered that adding more cement and less sand will improve extrudability⁶⁹. In this study, the S/C ratio was considered 1.7, and the maximum size of sand, 2.36 mm, was used. The length of extruded filaments for each mixture was measured, and the extrudability of the mixtures was compared in terms of the length of the extruded filament (Fig. 9). The fiber aspect ratio and volume fraction in mixtures are the primary factors determining the loss of workability in cement mixtures reinforced with natural fiber. However, due to the low content of fibers in the mixture, the workability and extrudability of the mixtures did not face any problems, and the mortars had good printing quality. Since the only difference between the mixtures is the type and percentage of fibers used, the comparison of the length of the extruded string of mortars and the surface of the print shows that increasing the percentage of fibers to 0.25% reduces the length of extruded mortar has surface defects. The use of cement substitutes such as GGBS and bentonite improves extrudability. On the other hand, the addition of fibers can affect the quality of the extruded mortar and make it difficult to pass through the nozzle when the fibers have the highest diameter. In contrast, the addition of fiber made the mix more cohesive. Thus, each printed layer was more stable and could better sustain its weight and that of the upper layers. Comparing the extruded length of different mixtures shows that the addition of fibers at the rate of 0.25% reduces the extruded length. Also, printed mortars will not have a fixed width. On the other hand, the mixtures containing 0.15% and 0.2% fibers had a higher extruded mortar length than the mixtures containing 0.1% fibers. At the same time, the mixtures with 0.15% and 0.2% by volume fibers almost had the same length in terms of extruded filaments. By comparing the effect of different fibers on the extrudability of the mixtures, it can be seen that the mixtures containing DPF and Coir had good printing quality due to the smaller diameter, and the highest extruded mortar length was measured for them. Although the mixtures containing CF and BF had good flowability, these mixtures performed weaker in extrudability and had the lowest length of extruded filaments. This can be attributed to the larger diameter of these fibers compared to other fibers. Also, mixtures containing 0.1%, 0.15%, and 0.2% PALF had the same extruded mortar length (300 mm), and this amount is the lowest (215 mm) for the F9-0.25PALF mixture (Fig. 9). However, adding these fibers to the mixtures did not have a significant adverse effect on the extrudability and all the mixtures passed the test. The extrudability of mixes is also influenced by their shear strength and dynamic yield stress. A very high shear strength means the mortar is stiff, which may not be extruded well or printed entirely. Very low shear strength also means the printed layer is too wet and not durable.

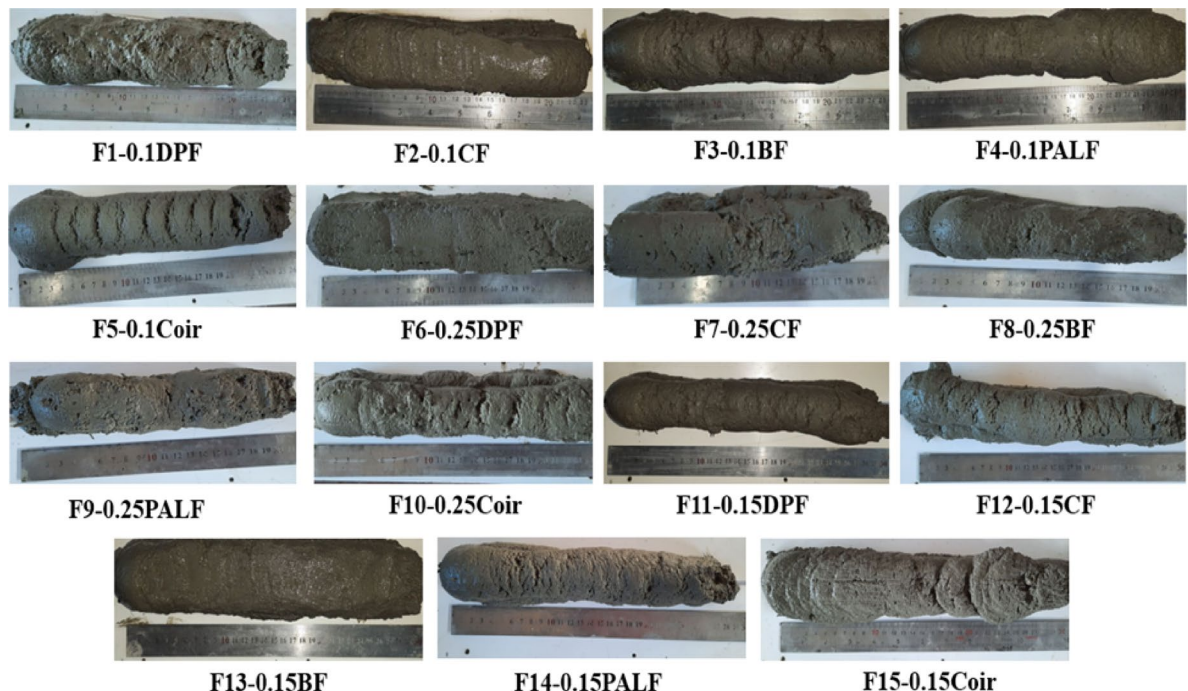


Fig. 8. Extruded filaments of some mixtures.

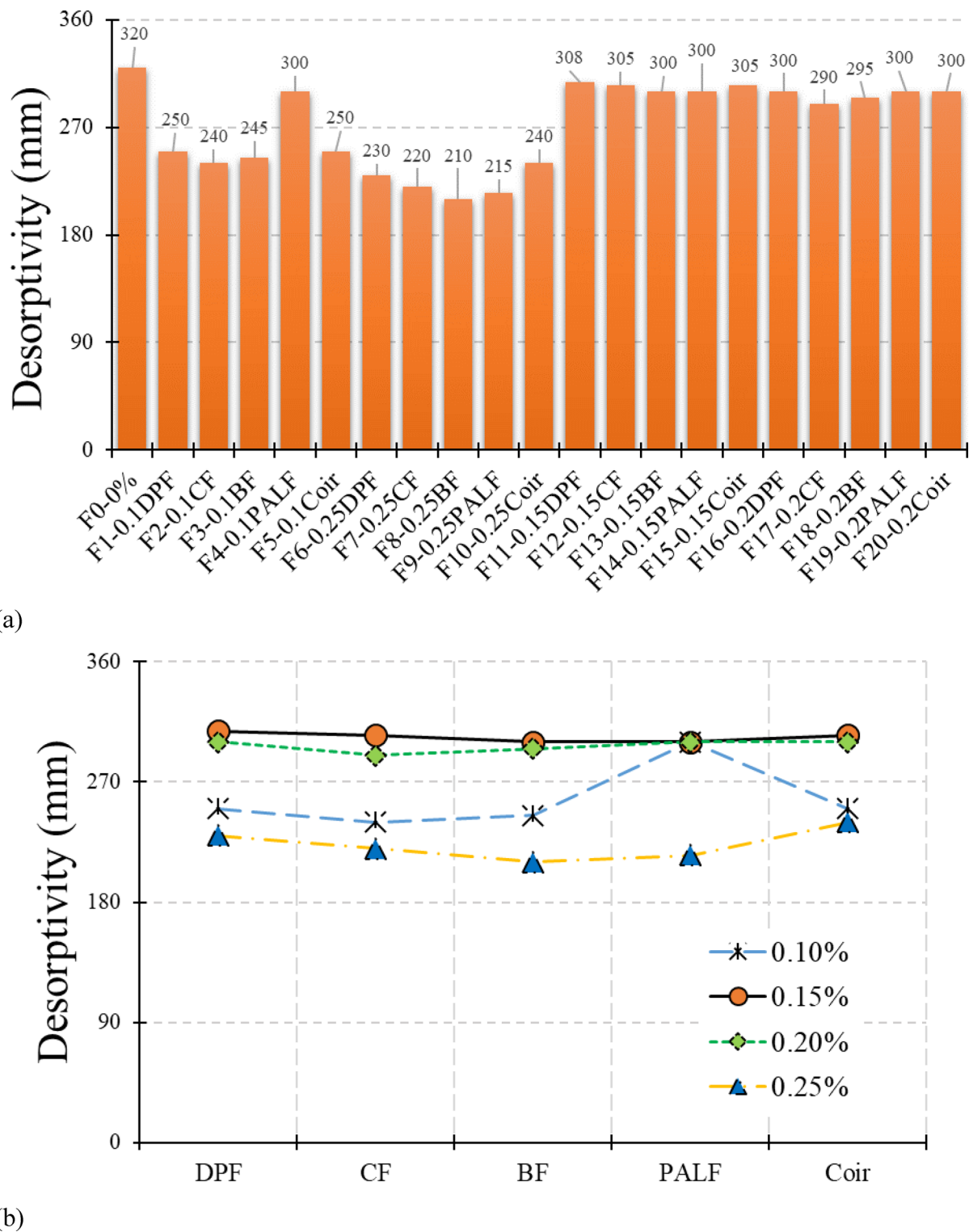


Fig. 9. Results of desorptivity test: (a) for all mixtures; (b) effect of volume fraction of recycled bio-waste fibers.

Buildability

Figure 10 shows the buildability test for mixtures before collapse. The mixtures were compared with each other in terms of the total number of plates that could be placed on them (Fig. 10). To evaluate the shape stability of mortars, the total height of the sample was measured after placing the last plate before collapsing (H_1). The closer this height is to the initial height of the sample ($H_0 = 50$ mm), or in other words, the closer the H_1/H_0 ratio is to 1, it means the buildability and maintain the shape is better. This ratio is “drop height ratio (DHR)”. Figure

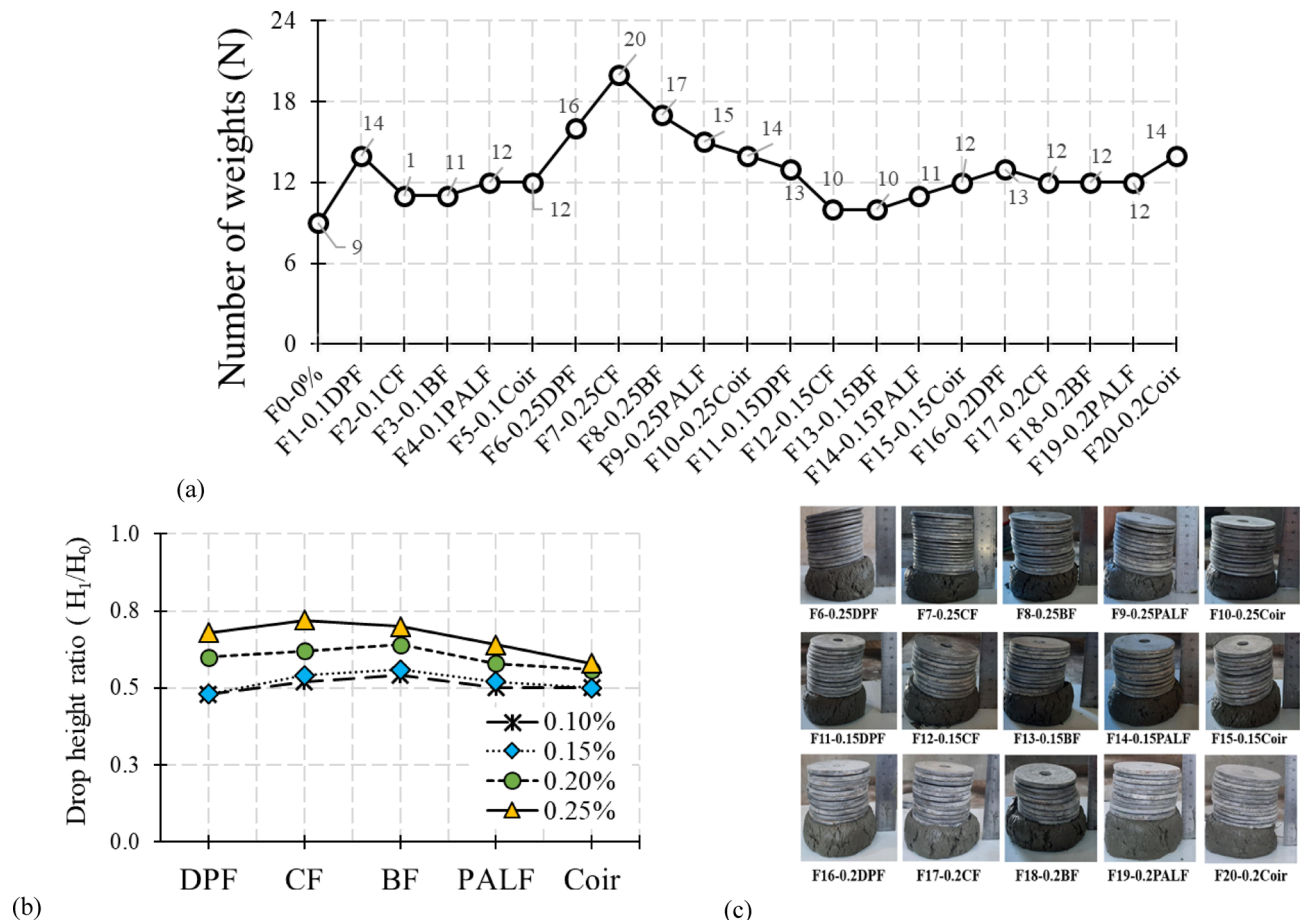


Fig. 10. Results of buildability test: **(a)** number of weights; **(b)** effect of volume fraction of recycled bio-waste fibers; **(c)** Shape stability of mixtures after final weight.

10 shows the drop height ratio for the fibers used in the mixtures with different percentages. Therefore, a mixture with high buildability is a mixture that can bear a large number of weights before collapse and has the least deformation due to the weight of the upper layers on it. In general, adding SCMs and powder materials to the mixture improves the buildability of a 3D printable mixture, but it can reduce the workability. The buildability of 3DPC is influenced by various aspects, including fibers, SCMs, aggregate content, aggregate size, and rest time. The shorter the rest time, the higher the bonding strength between layers. Another influencing factor is the amount of aggregate in the mortar⁷⁰. The higher the sand content, the better the buildability and shape retention, but it may make extrudability difficult. The addition of fibers reduces the shrinkage and cracking in the plastic state as well as increases the yield stress of the material and it makes the mortar have enough cohesiveness for the layered structure. It should be noted that the yield stress of fresh concrete is the main parameter that determines the shape stability before setting. The material with the high yield stress shows sufficient buildability with less deformation and an increasing load⁷¹. By comparing the number of weights that each mixture can bear before collapsing, it shows that adding fibers at the rate of 0.1% by volume increases this number from 9 (for F0-0%) to 14 and for 0.2% fibers to 20 in the best case. The number of weights for mixtures containing 0.1%, 0.15%, and 0.2% fibers is almost close to each other, and this number is the highest for mixtures containing 0.25% fibers. Similarly, by examining Fig. 10, it is clear that adding 0.1% of fibers to the mixture increases the drop height ratio to 25% compared to the mixture without fibers. This ratio increases up to 80% by adding 0.2% of fibers to the mixture. Therefore, mixtures containing 0.25% natural fibers have a larger drop height ratio and closer to 1 than other percentages of fiber addition. By examining the effect of the type of fibers, it was found that there was no significant difference between different natural fibers in the buildability of a 3D printable mixture. However, BF and CF have a larger DHR and showed higher shape stability due to their larger diameter compared to other fibers and the larger space occupy in the mixture.

Open time

The duration of fresh concrete that retains good printability is known as the “open time”. Once disruption occurs in the extrusion process of filaments, the open time is assumed to have ended. Figure 11 shows the extruded filaments at different rest times for F0-0% and F18-0.2BF mixtures. To investigate the effect of different fibers on the rest time of the mixtures, the length of the extruded filaments was measured at different times. The length of the initial design was 25 cm, and with the passage of time, a smaller length was extruded from each mortar. The

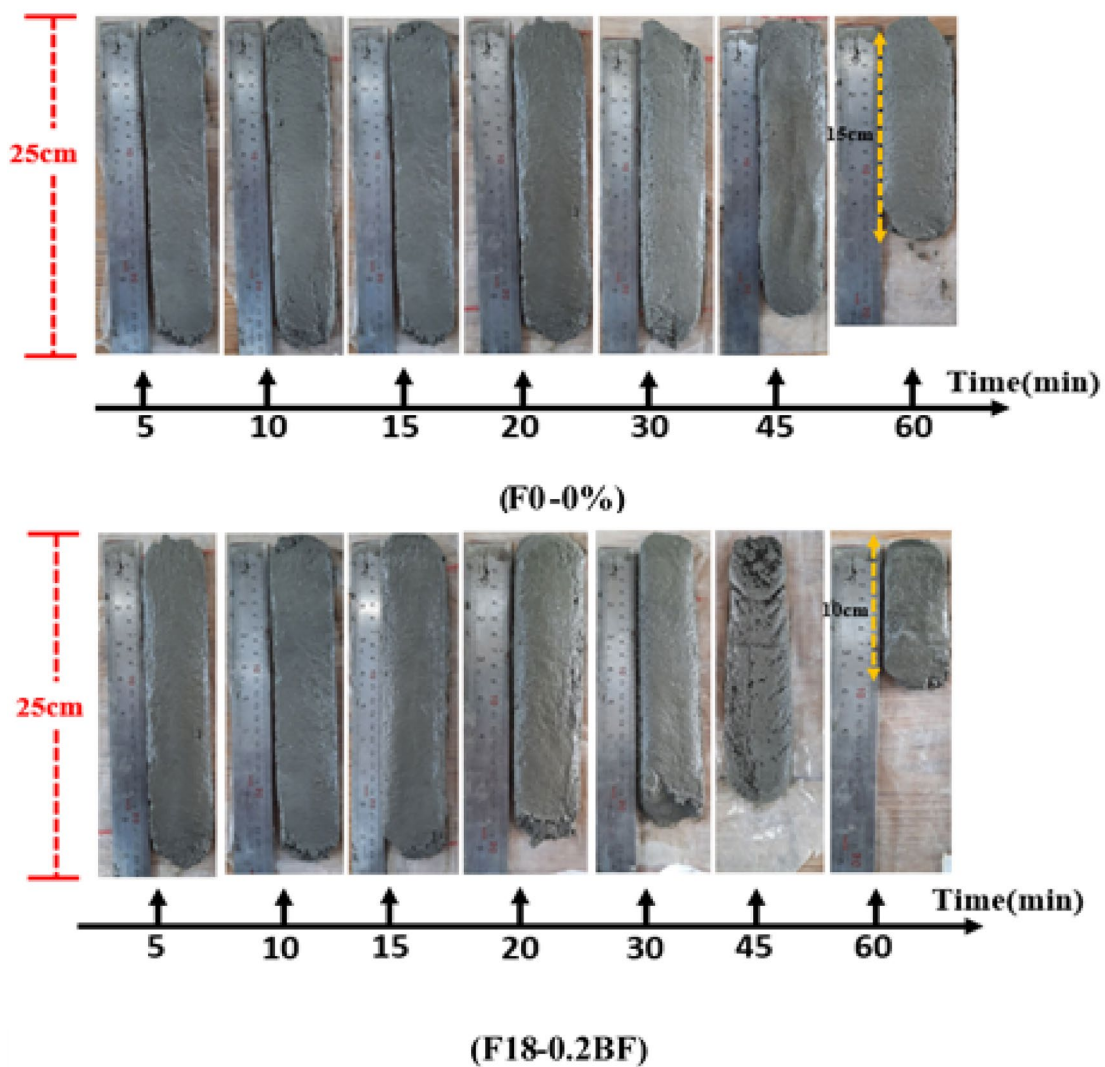


Fig. 11. Extruded filaments of F0-0% & F18-0.2BF mixtures at different rest times.

results of the open-time test for mixtures containing 0.2% fibers are shown in Fig. 12. A crucial related concept is the initial setting time of concrete. Adding natural fibers to the mixture can reduce the resting time of the extruded filaments. Higher fiber dosage increases the buildability but decreases the possible open printing time. Utilizing pre-treated fibers with minimal lignin content in cement composites may also lessen the detrimental impact of plant-based natural fibers on cement hydration. Moreover, adding more chemical accelerators and high-surface-area supplementary materials to mixtures, like limestone powdered that has been finely ground, may also improve early-age hydration. The results showed that all the mixtures had problems extruding after 60 min, and the extruded length decreased after 30 min. However, in the mixture without fibers, the extruded length was 15 cm in 60 min, and this length reached 10 cm for the mixture containing 0.2% of fibers. This is attributed to the presence of pectin's in some of these fibers, which act as a calcium silicate (CSH) growth inhibitor. Until the 15th minute, all the mixtures had a total length of 25 cm, but after the 20th minute, the length of the mixtures containing fibers decreased (less than 25 cm). After 60 min, it was the first time no concrete could be removed from the nozzle. The F18-0.2BF mixture had the lowest length compared to the mixtures containing other fibers at various times. This can be considered due to the larger diameter of BF compared to other fibers.

Compressive strength

The compressive strength of casting specimens with different natural fibers with different volume fraction percentages at the ages of 1, 7, and 28 days is shown in Fig. 13. Replacing cement with materials that increase resistance helps to achieve an optimal design with high strength and low CO₂ emissions. Adding more than the amount of bentonite and LP as a substitute for ordinary Portland cement will reduce the compressive strength of the samples. All mortars have the same W/C and S/C ratio. For all the fiber types, an enhancement of the mechanical strength is observed. The compressive strength of “F1-F5” mixtures increased up to 20%, and “F11-F20” mixtures increased to 26% and 28%, respectively, compared to the mixture without fibers (F0-0%).

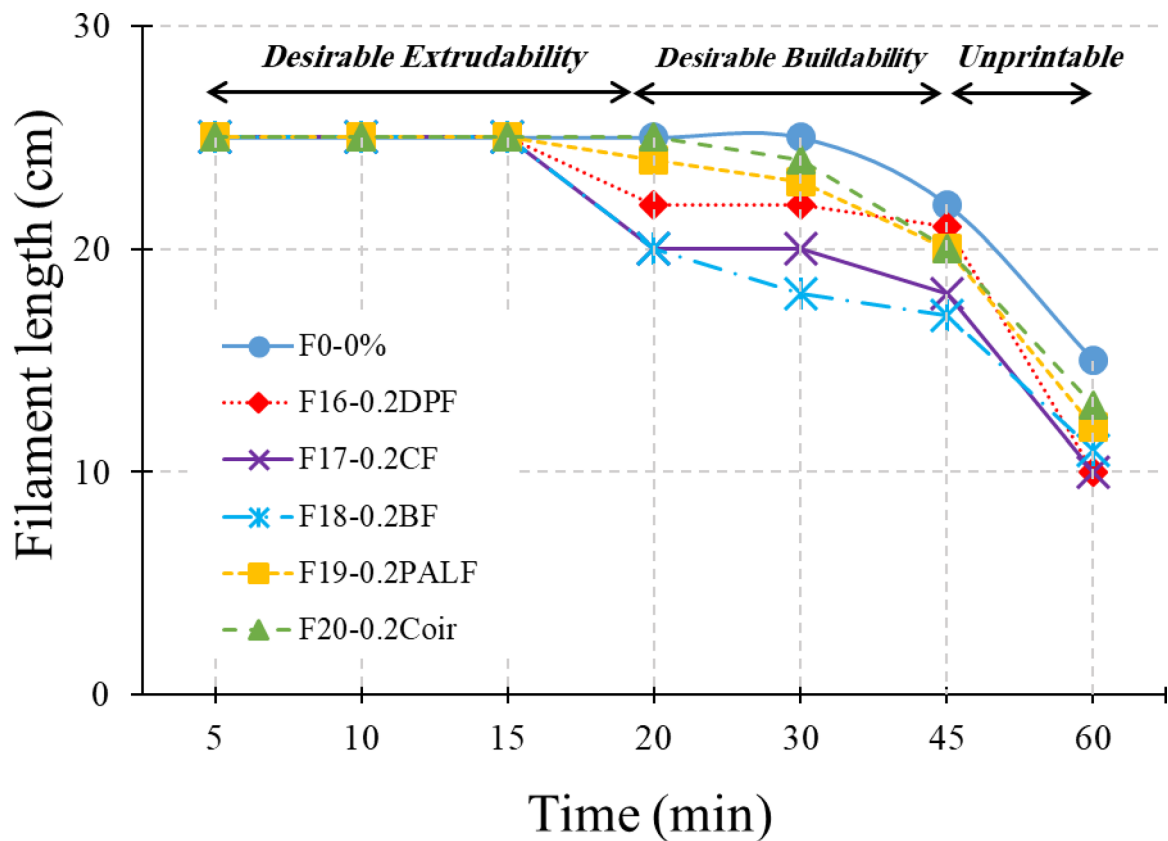


Fig. 12. Filament length of some mixtures with different rest time.

However, adding more fibers to the mixture (0.25% vol) did not significantly increase the compressive strength, and less than 0.2% of the fibers were observed in most of the mixtures. This behavior was observed because of the formation of voids due to the excess fiber content in concrete. By comparing different fibers, the addition of DPF by 0.2% showed an increase in compressive strength by 15% and 25% for 7 and 28 days, respectively. This value was obtained for the “F20-0.2Coir” mixture of 12% and 28%. This can be attributed to the uniform distribution and smaller diameter of these fibers compared to others. Also, adding other investigated fibers at 0.2% by volume has significantly increased the compressive strength. Adding 0.2% and 0.15% fibers for almost all mixtures had the highest compressive strength. However, for the mixtures containing PALF, the increase in the percentage of fibers has been accompanied by a decrease in compressive strength, and the “F4-0.1PALF” mixture has the highest compressive strength. 3DPC shows anisotropic behavior. Therefore, it is essential to determine the direction-wise compressive strength of the 3D printable objects. The printed samples were subjected to compressive strength tests in three loading directions. Since the mixtures containing 0.15% and 0.2% fibers had the best performance in the compressive strength of the cast samples, these mixtures were subjected to compressive strength tests in the printed state. The results of the compressive strength test of printed samples in three loading directions at the age of 28 days are shown in Fig. 13. The casted samples show a higher compressive strength than the 3D printed specimens. The reason for this is the presence of mold and compaction in casting specimens compared to printed ones. The highest compressive strength was related to loading in the direction perpendicular to the print (Z direction). This was also observed in previous research^{17,72–74}. Loading in the X and Y directions had almost the same compressive strength. Extruded samples in the print and lateral directions change their shape due to the lack of molding with the least applied pressure and show less compressive strength. Adding high volume percentage of fibers in the printed samples can slightly reduce the compressive strength. The results show that the mixtures with 0.2% fibers showed lower compressive strength than those with 0.1% fibers. Because the fibers oriented in the direction of loading behave like the voids. Similarly, the results were also shown by Hambach et al.⁷⁵, for a fiber content of 1 to 3% of changes, leading to a 20% reduction in compressive strength. Also, similar to the casting specimens, DPF and Coir mixtures showed higher compressive strength than mixtures containing other fibers in all three directions. For example, the “F11-0.15DPF-Printed” mixture has 28% and 39% higher compressive strength in the Z direction than the “F13-0.15BF-Printed” and “F14-0.15PALF-Printed” mixtures, respectively. This increase in the amount for the “F15-0.15Coir-Printed” mixture is 27.5% and 35%, respectively. The lowest compressive strength was related to mixtures containing BF and PALF fibers. This is because the larger diameter of these fibers in concrete creates space, and the gap between the fibers and the matrix is visible.

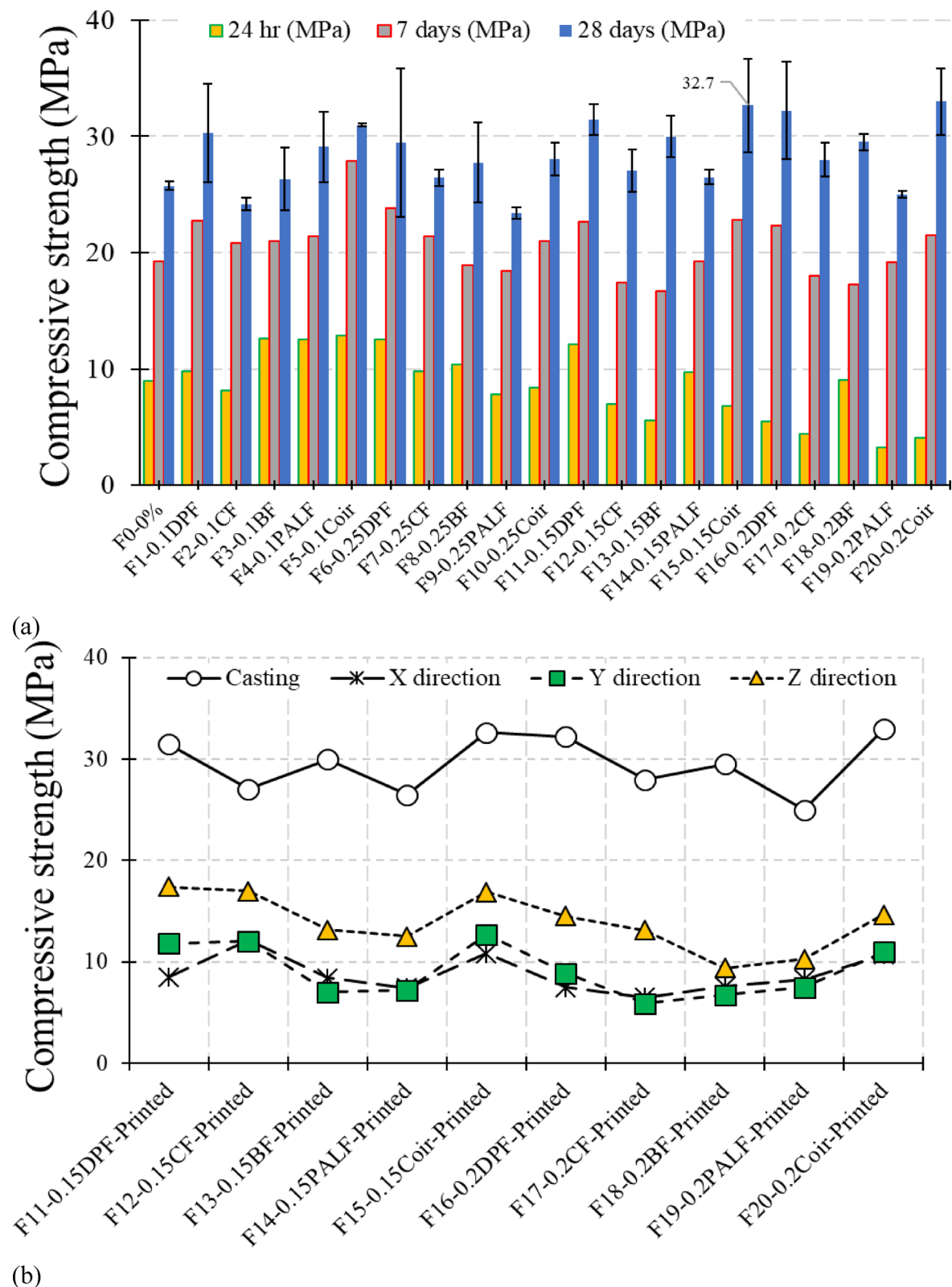


Fig. 13. Results of compressive strength test: (a) casted specimens; (b) printed specimens at age of 28 day.

Tensile strength

Figure 14a shows the direct tensile force of mixtures. Also, normalized results by compressive strength results is illustrated in Fig. 14b. Overall, the results show that the use of natural fibers increases the tensile strength so that the mixtures containing 0.1% fibers up to 46% and 0.2% fibers up to 66% improvement in tensile strength. The

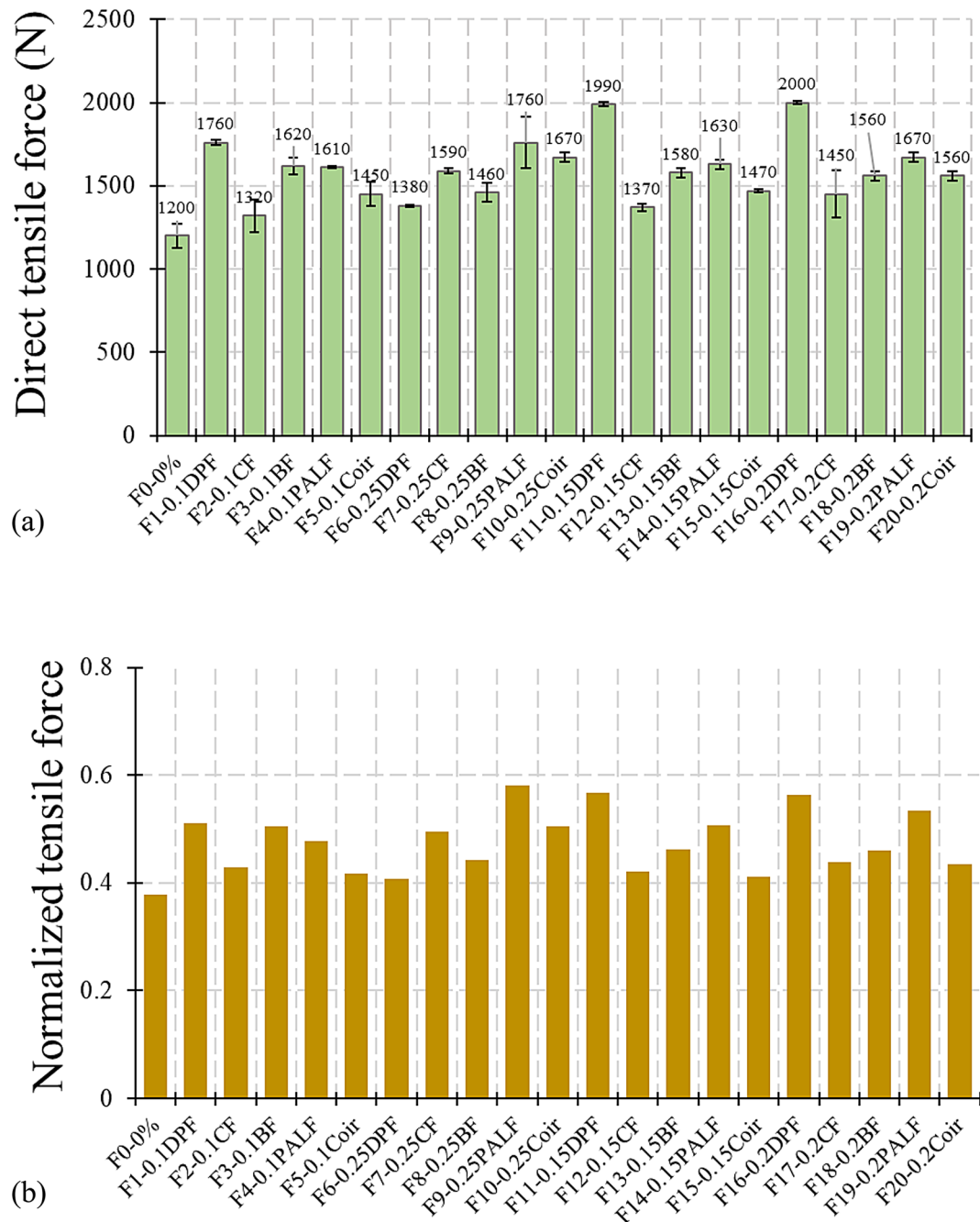


Fig. 14. Results of direct tension test for all mixtures: **(a)** direct tensile force; **(b)** normalized results by compressive strength.

use of natural fibers increases tensile strength due to factors such as high cellulose content, improved fiber-matrix interaction, and treatment processes that enhance fiber surface morphology and mechanical properties. The increase in tensile strength for some fibers did not have a clear trend. Mixtures containing DPF and BF did not significantly increase tensile strength by adding 0.25% fibers. It was even lower than the mixture with 0.1% fiber. This is because the availability of fibers on the layer surface creates more pores in the concrete. With the increase in fiber content, the void percentage of the mixture increases, thus reducing the strength of the tensile bond. Adding 0.2% fibers for these mixtures had the best results in the direct tensile test. On the other hand, mixtures containing CF, PALF, and Coir had higher tensile strength and increased fiber percentage. Because these fibers are flexible and can create bridges between layers and improve adhesion between layers. Also, the use of coconut and pineapple leaf fibers increases tensile strength due to their high cellulose content, crystallinity, and the effectiveness of surface treatments that enhance fiber-matrix bonding and mechanical properties⁷⁶. For example, the “F9-0.25PALF” mixture enhances the direct tensile strength by about 10% compared to the mixture “F4-0.1PALF”. Natural fibers from pineapple leaves are a good choice for study because of their high tensile strength

and high cellulose content. Also, date palm fibers have good tensile strength due to their ability to strengthen the fiber-matrix bond, the positive effects of chemical treatments, and the inherent high tensile strength. For instance, adding 0.2% of DPF in the mixture (F16-0.2DPF) has a higher tensile strength than adding 0.2% of BF, CF, and Coir, which is 25, 37, and 28%, respectively. In the case of banana fibers, the results show that a lower fiber dosage significantly affects the tensile strength, while a higher dosage decreases the tensile strength. For example, mixture “F3-0.1BF” has 2.5, 3.8, and 10.9% improvement in tensile strength compared to “F13-0.15BF”, “F18-0.2BF” and “F8-0.25BF” mixtures, respectively. This can be attributed to the larger diameter of these fibers and the creation of space in the concrete.

Pull-out bond strength

Fiber pull-out behavior depends on a number of variables, such as mechanical resistance, friction, and physiochemical stickiness. The interfacial bond strengths obtained from briquette pull-out tests for natural fibers incorporated into 3D printable mortar were obtained and compared with each other. The maximum load when pulling out the fibers was measured individually. The bond strength for each fiber was calculated according to Eq. 1 and the results are shown in Fig. 15. The resistance and pull-out behavior of fibers can be assessed using a variety of measures. A crucial metric for evaluating the performance of fibers in concrete is the maximum fiber stress. The fiber will fracture prior to full pull-out if the maximal stress exceeds its tensile strength.

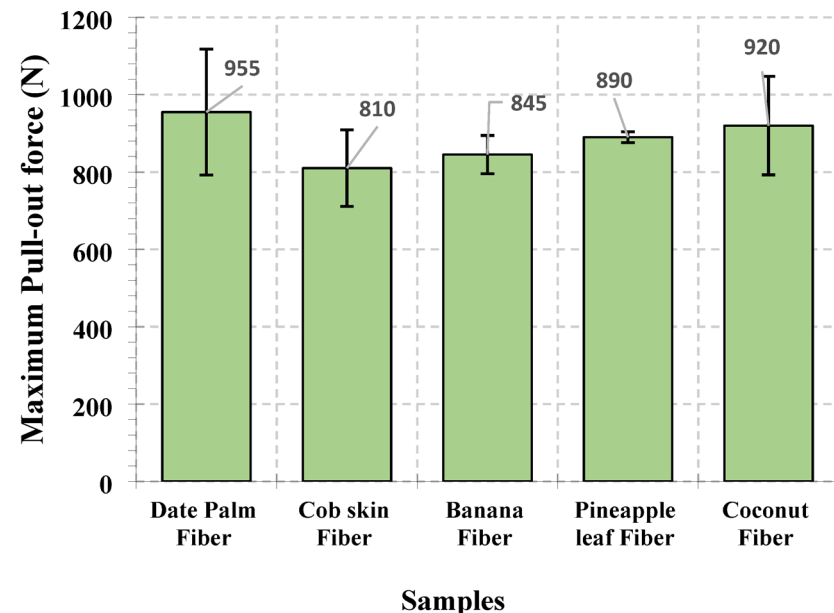
Date palm and coconut fibers exhibit the highest bond strengths, likely due to their smaller diameter and lignocellulosic composition and surface roughness, which promote mechanical interlocking and frictional resistance at the fiber-matrix interface. Such characteristics enable effective stress transfer, minimizing slippage under shear loading. Date palm and coconut, with higher lignin content, offer enhanced rigidity and matrix compatibility, fostering stronger bonds through improved wetting and adhesion during hydration. In contrast, banana and pineapple leaf fibers, may absorb more water, creating micro-voids at the interface that compromise bond integrity. The bond strength results for the fibers are consistent with the direct tensile test results of the samples, where the highest direct tensile force was for samples containing date palm, coconut, and pineapple leaf fibers. Date palm and coconut's superior adhesion enables effective crack arrest, elevating tensile performance. This relationship underscores bond strength's pivotal role in mechanical efficacy, as weaker interfaces would precipitate fiber pull-out, reducing overall composite integrity. Different failure modes were observed during pull-out test. In date palm, coconut, and pineapple leaf samples, the failure mode was pull-out fiber where in the fibers remained intact post-failure, continuing to connect the two halves of the briquette despite the matrix fracturing. This suggests a failure mode dominated by matrix cracking or interfacial debonding rather than fiber rupture. In contrast, cob skin and banana fibers underwent simultaneous failure alongside the mortar, indicating a combined fiber-matrix fracture, likely due to lower tensile capacity or weaker interfacial adhesion under shear loading.

Flexural strength of 3D-printed beams

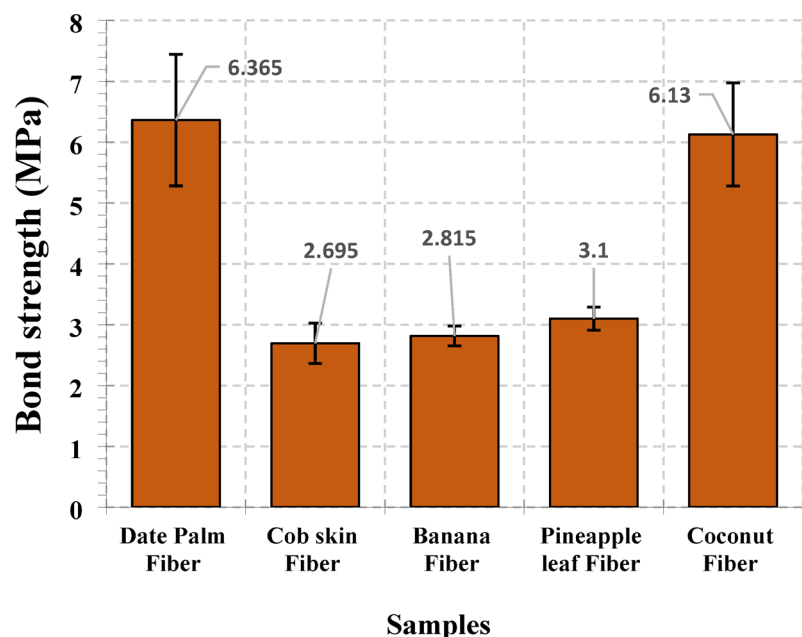
A flexural strength test was performed on casting specimens with dimensions $40 \times 40 \times 160$ mm. The flexural strengths of specimens with different natural fibers at the age of 28 days and normalized results by compressive strength are shown in Fig. 16. In general, adding cement substitutes such as GGBS and bentonite can improve the flexural strength of the mixture. Also, keeping the S/P ratio constant = 1.2 results in better performance in bending. As the S/P ratio increases, the fresh mix hardens and cannot be printed well, decreasing flexural strength. Also, adding fibers, regardless of type, can improve bending force. Adding fibers delay the initiation and coalescence of cracks under tension and flexure, creating the “bridge effect” phenomenon. As shown in Fig. 16, adding date palm fibers by 0.25% improves the flexural strength by 25%. Also, adding CF, BF, and PALF to the mixture up to 0.25% increased by 18, 24 and 28%, respectively, compared to the mix without fibers. On the other hand, the addition of more content of coconut fibers slightly reduced the flexural strength, so the mixture with 0.1% Coir showed 18.5% more flexural strength than the mixture containing 0.25% Coir. This can be attributed to the increase in twisted fibers and the creation of voids in concrete due to the increase in fiber content.

Similar to the compressive strength, the loading direction is effective in bending force. The samples printed in two layers, according to Fig. 6, were subjected to bending tests in the Y and Z directions. Mixtures containing 0.15% and 0.2% fibers were evaluated. The flexural strength results of the printed samples are shown in Fig. 17. Printed samples showed different bending forces in different loading directions compared to cast samples. In general, the ultimate bending force of the printed filaments was lower than that of the cast specimens, except for the mixtures containing coconut fibers, which had higher flexural strength than the cast samples, which were 10% for 0.15% fibers and 15% for 0.2% fibers. However, the samples tested along the Z direction (perpendicular to the print) showed higher bending force than the Y direction (lateral direction) due to better fiber orientation and less porosity. In all the mixtures, the tested samples along the Y direction had the lowest flexural strength. This is mainly due to the poor interface of the printed filaments, which are aligned in the direction of loading. For example, the ultimate bending force of mixtures “F11-0.15DPF”, “F12-0.15CF”, and “F15-0.15Coir” in the Z direction is 7%, 20%, and 44% higher than this force in the Y direction, respectively. Almost the same values were obtained for mixtures “F13-0.15BF” and “F14-0.15PALF” in both directions. Also, similar results were observed for mixtures containing 0.2% of fibers (F16 to F20). Similar to the samples with the mold, increasing the fiber content increases the final bending force in the printed samples. The presence of fibers can bridge the crack surfaces and delay beam failure. However, increasing the pineapple leaf fiber (PALF) content in the mix will disrupt the smooth extrusion, creating more voids and thus slightly reducing the strength.

To investigate the effect of the delay between the printed layers, the flexural strength of the mixtures “F0-0%” and “F16-0.2DPF” was evaluated by changing the time interval between the printed layers such as 5 min, 1 h, 2 h, and 3 h. The longer the time interval between the layers, the lower the bending force, and the lower the print



(a)



(b)

Fig. 15. Results of pull-out test: (a) maximum pull-out force (P_{\max}); (b) bond strength.

speed and nozzle distance, the better the effect. This has also been observed in the results of other researchers. The results of the delay effect on flexural strength are shown in Fig. 17b. As the time gap increases, the strength of the bond between the layers decreases and reduces the flexural strength. The results showed that increasing the time gap of 3 h between the layers decreases the ultimate bending force in the Z direction for “F0-0%” and “F16-0.2DPF” mixtures by the amount of 1530 N and 1360 N, respectively. However, adding 0.2% fibers improves the flexural strength by 20% compared to the mix without fibers. The extruded filaments and failure modes of the samples are shown in Fig. 18. As can be seen, for a short time interval (5 min), the small crack initiates at the bottom of the sample. In contrast, for a considerable interval of time (3 h), the straight large vertical crack occurs. However, all cast and printed samples had brittle behavior in flexural failure. This is because of the bonding between fibers and the matrix, the orientation and load distribution during testing, and the small volume of

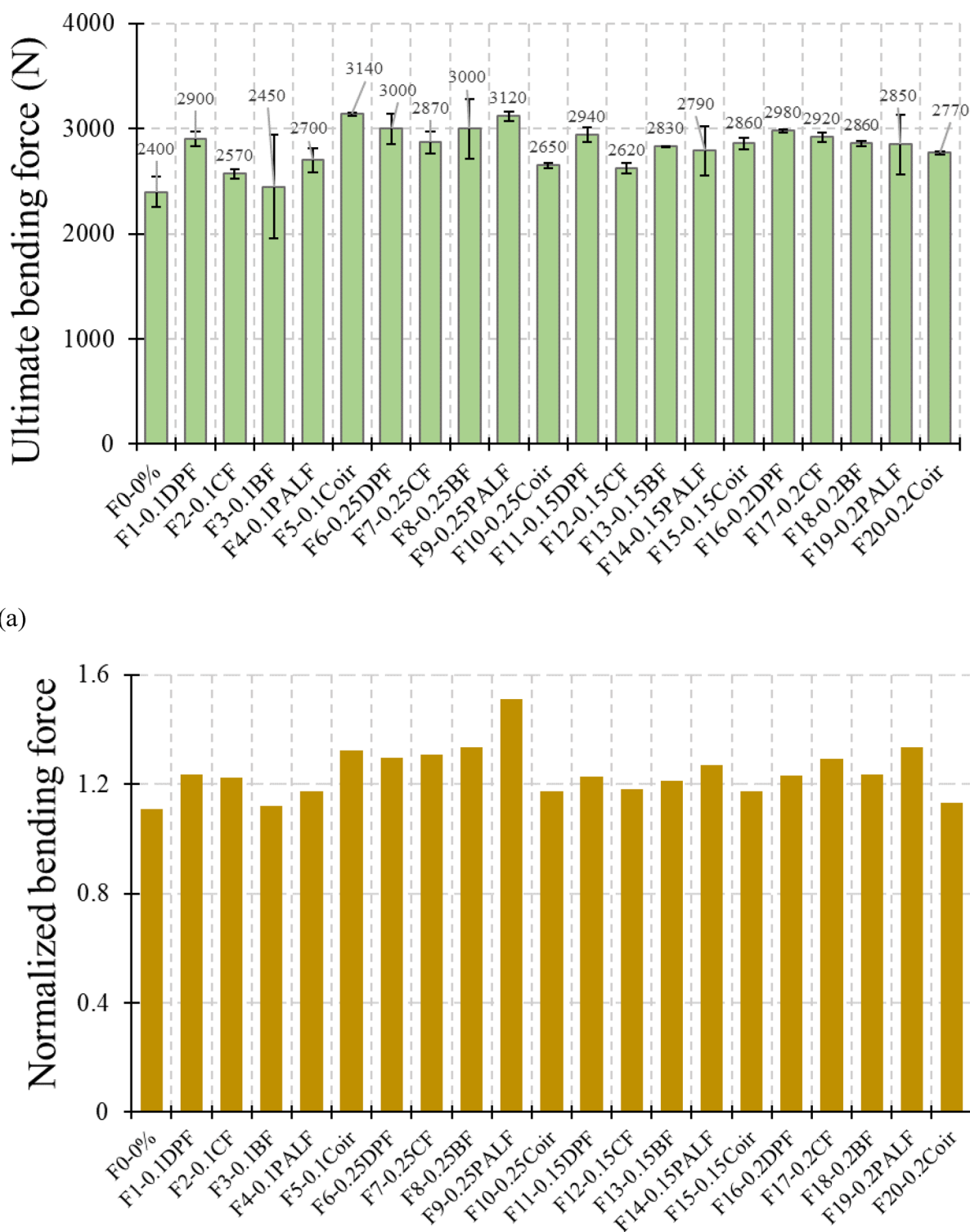


Fig. 16. Results of flexural test for cast samples: **(a)** ultimate bending force; **(b)** normalized results by compressive strength.

fibers in the mixture. Figure 19 shows the debonding of natural fibers from the matrix and the effect of fibers in the sample during failure.

By comparing the different percentages of fibers in the mixture in terms of rheology and strength, 0.2% was chosen as the optimal percentage, and the cast and printed samples containing 0.2% fibers with dimensions of 10cmx10cmx50cm were subjected to the four-point bending test according to the ASTM C1609 standard²⁷. The

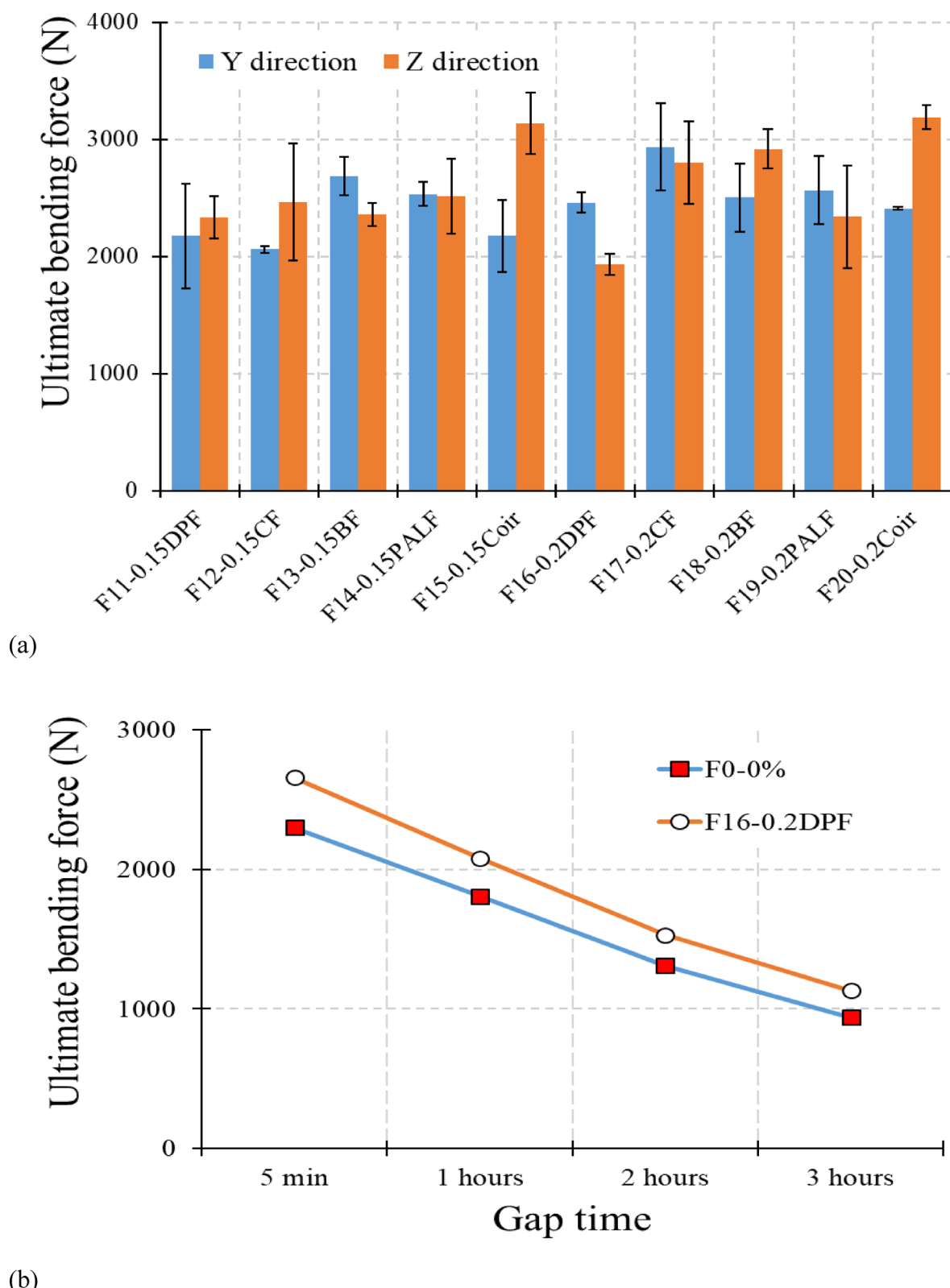


Fig. 17. Results of flexural test: **(a)** printed samples without gap time; **(b)** printed samples with different gap time.

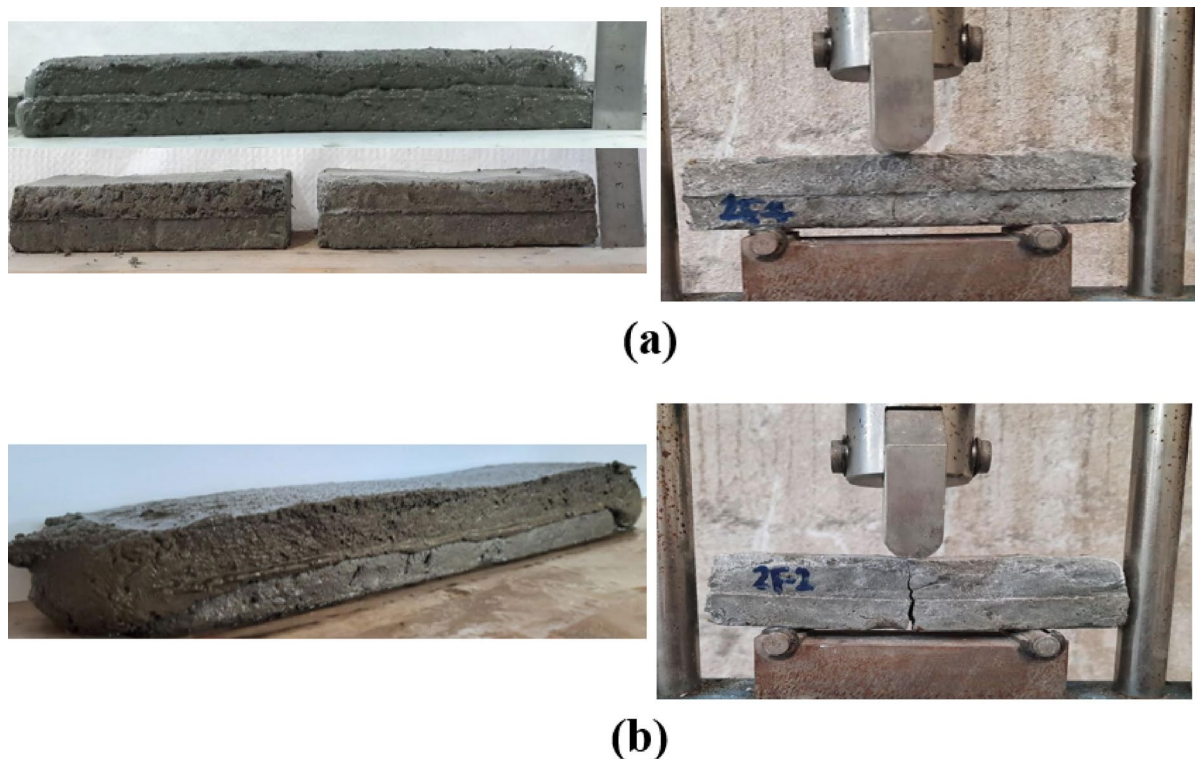


Fig. 18. Extruded filaments and failure modes of samples: (a) with 5 min gap time between two layers; (b) with 3 h gap time between two layers.

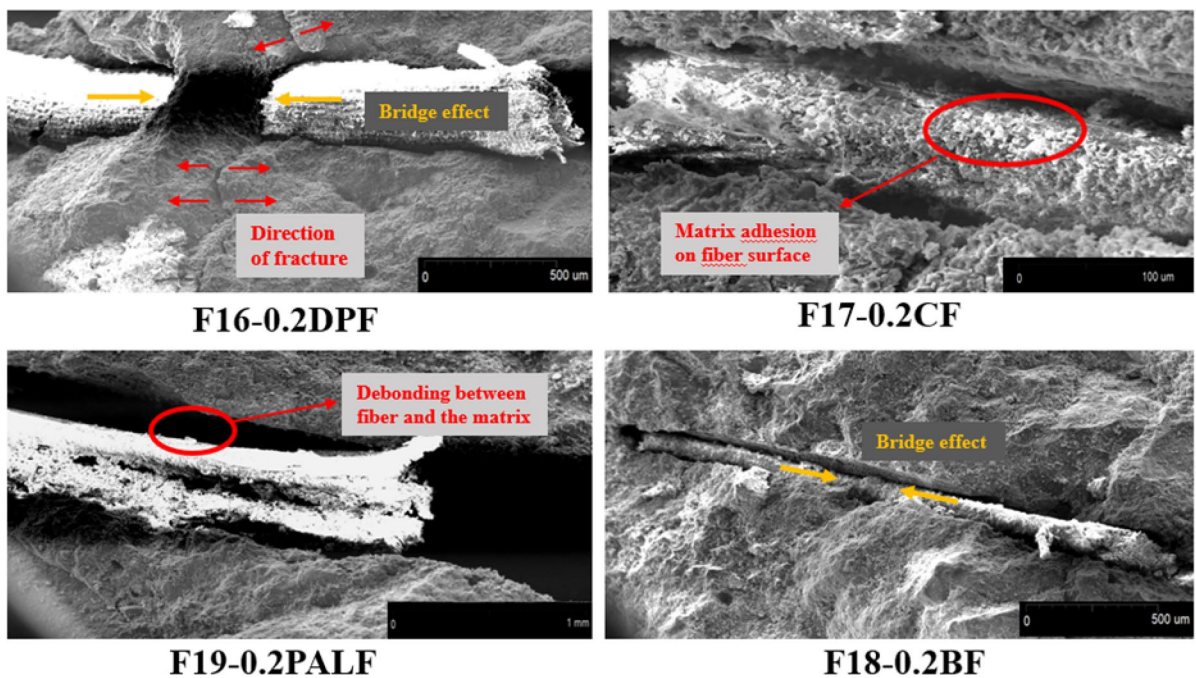


Fig. 19. SEM images of action mechanism of fibers in PFRCS.

beam flexural test was performed with a Universal hydraulic servo-controlled machine with 600kN capacity, as shown in Fig. 20. Figure 21 illustrated the typical load-deflection curves of mold-cast and printed samples with 0.2% fiber content. The results showed that the addition of fibers delays the bending failure by creating a bridge effect (As shown in Fig. 19). The addition of CF, BF, and PALF improves the ultimate bending force by 15%, 37%,

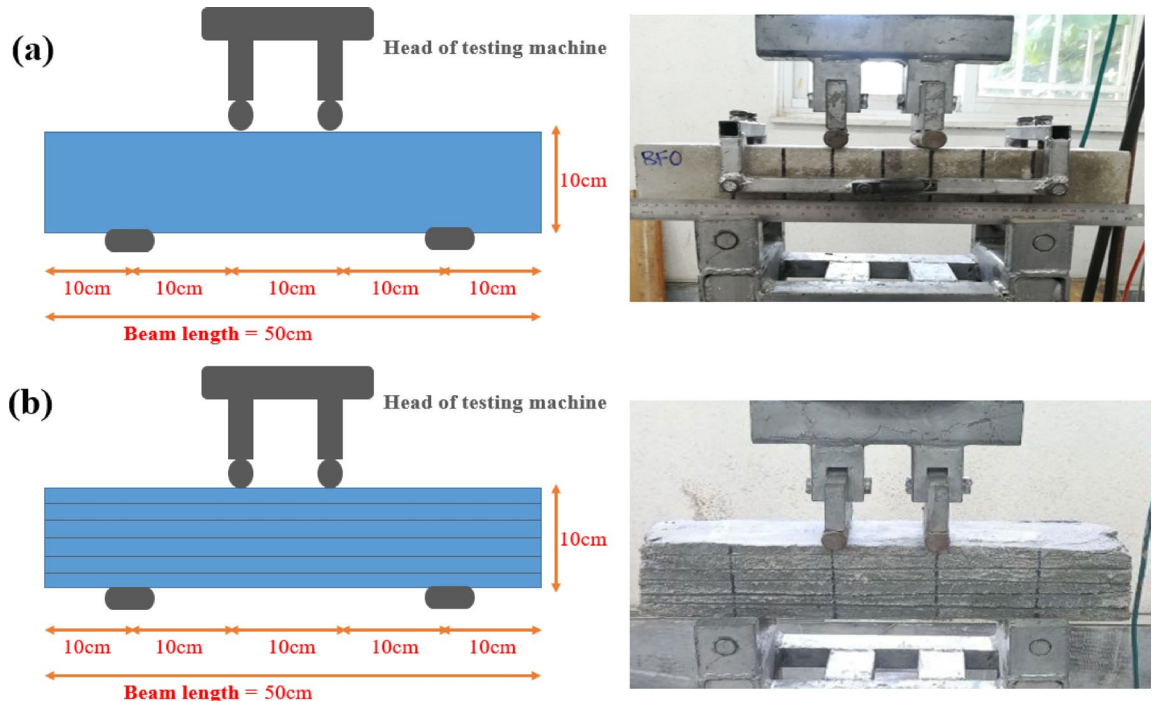


Fig. 20. Flexural test of large-scale samples: **(a)** mold-cast sample; **b**) 3D printed sample.

and 19%, respectively, compared to the mixture without fibers in casting samples. However, adding date palm and coconut fibers slightly reduced the flexural strength in the sample with the mold. For the printed beams loaded in the Z direction, the ductility was clearly increased compared to the cast samples. The layered structure of the printed samples allows them to absorb significant energy, which could help a lot in the enhancement of flexural deformability and energy dissipation. Also, for all mixtures, due to the better orientation of the fibers, the flexural strength of the printed beams was higher than that of the cast beams. This was also observed in previous studies where printed samples showed superior flexural performance over molded samples due to fiber alignment in the printing direction⁵¹. For example, printed samples from 3.2kN to 11kN improve the ultimate bending force. Previous studies have also reported an increase in bending strength in beams containing natural fibers. For instance, kenaf fiber-reinforced polymer (KFRP) laminates increased the ultimate load of reinforced concrete beams by 77.9% compared to control beams⁷⁸. Similarly, other studies have shown improvements in load capacity when using fiber-reinforced polymers (FRPs)⁷⁹. Also, higher ultimate strain was obtained compared to cast beams. This is because the printed layers are placed in the path of the crack, causing a delay in crack propagation and flexural failure. The highest flexural strength is related to the “F17-0.2CF” printed beam due to the strong surface connection and adhesion of fibers and matrix, which has 41.6%, 31.5%, and 16.6% improvement in the ultimate bending force compared to the mixtures “F18-0.2BF”, “F19-0.2PALF”, and “F20-0.2Coir”, respectively. Also, the highest strain was for the mixture “F17-0.2CF”, which is 1.8 mm. Figure 22 shows the typical failure pattern of flexural samples. As mentioned earlier, the cast and printed samples had a brittle failure, and the first crack in the beams was equal to the last crack. This can be attributed to the low weight of fibers and debonding of fibers and matrix.

The summary of the findings of the present study is shown in Table 4. The best mixtures for each test were determined. In general, adding higher fiber content leads to a reduced flowability and open time of the mixtures. In contrast, it improves the buildability (F6, F7 and F8). For the extrudability and printability tests, mixtures with 0.15 and 0.2 vol% of fibers have acceptable results. Also, by comparing the results of the hardened samples, it was found that the addition of fibers increases the compressive strength, direct tensile strength and ultimate bending strength. However, adding higher fibers content (0.25 vol%) will reduce the mechanical strength of the sample due to the creation of voids in the surface of the printed samples, and mixtures containing 0.2 vol% of fibers showed the highest mechanical strength.

Conclusions

This study evaluated added five types of natural fibers derived from plants in four different percentages of 0.1, 0.15, 0.2, and 0.25% within 3D-printing concrete. Various fresh and mechanical tests were considered. The main findings of the present study are as follows:

- The addition of fibers decreased the flowability and slump of the mortar. However, due to the small size of the fibers and their small amount in the mixture, it does not cause problems with flowability.
- Increasing the percentage of fibers to 0.25% decreased length of extruded filaments. On the other hand, the mixtures containing 0.15% and 0.2% fibers had a higher extruded mortar length than the mixtures containing

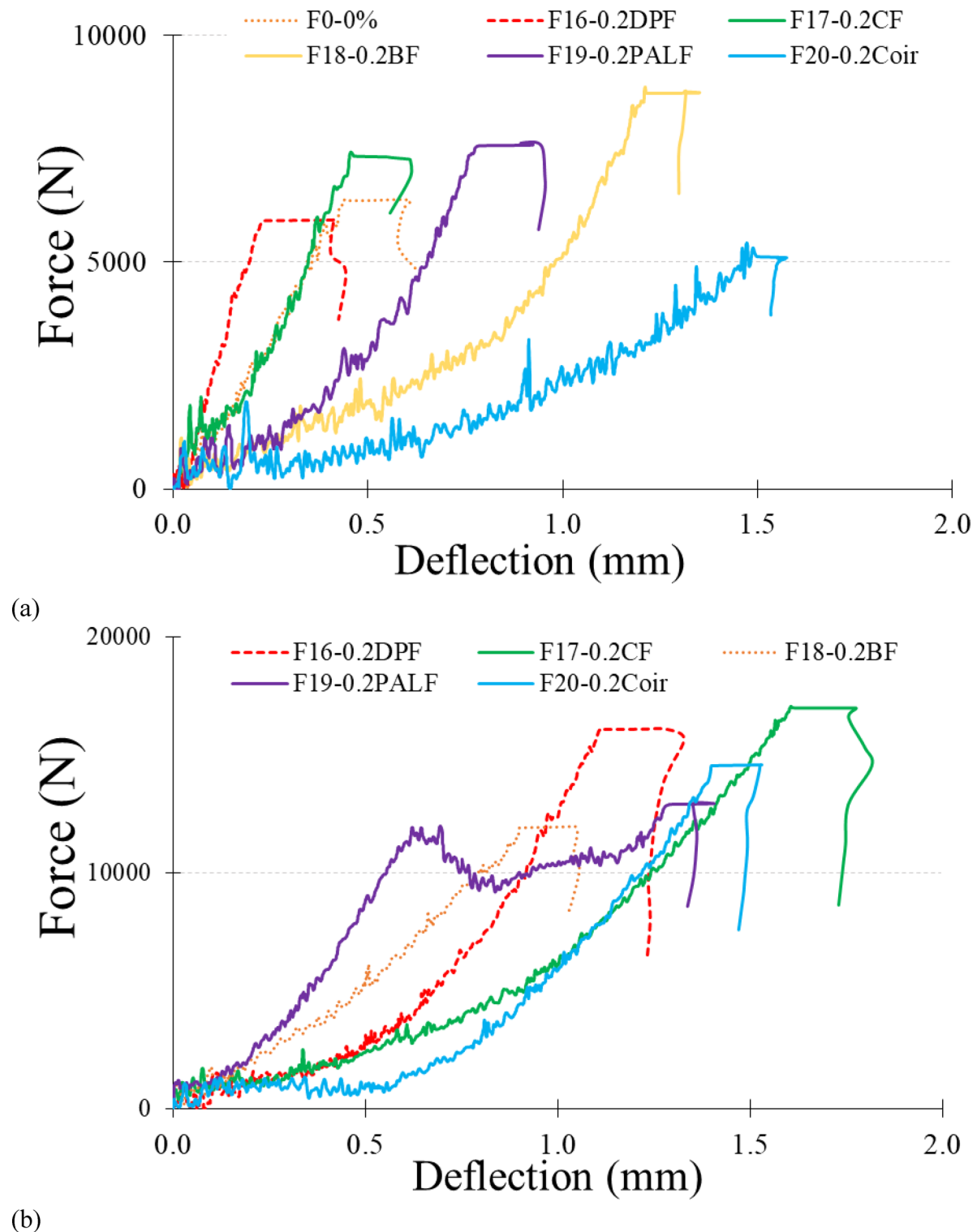


Fig. 21. Typical load–deflection curves of mold-cast and printed samples: (a) mold-cast samples; (b) 3D-printed samples.

0.1% fibers. The mixtures containing DPF and Coir had good printing quality due to the smaller diameter, and the highest extruded mortar length was measured for them.

- The longer the time interval between the printed layers, the greater the stability of the shape, but it may disturb the extrudability process. The addition of fibers reduces the shrinkage and cracking in the plastic state as well as increases the yield stress of the material and it makes the mortar have enough cohesiveness for the layered structure.

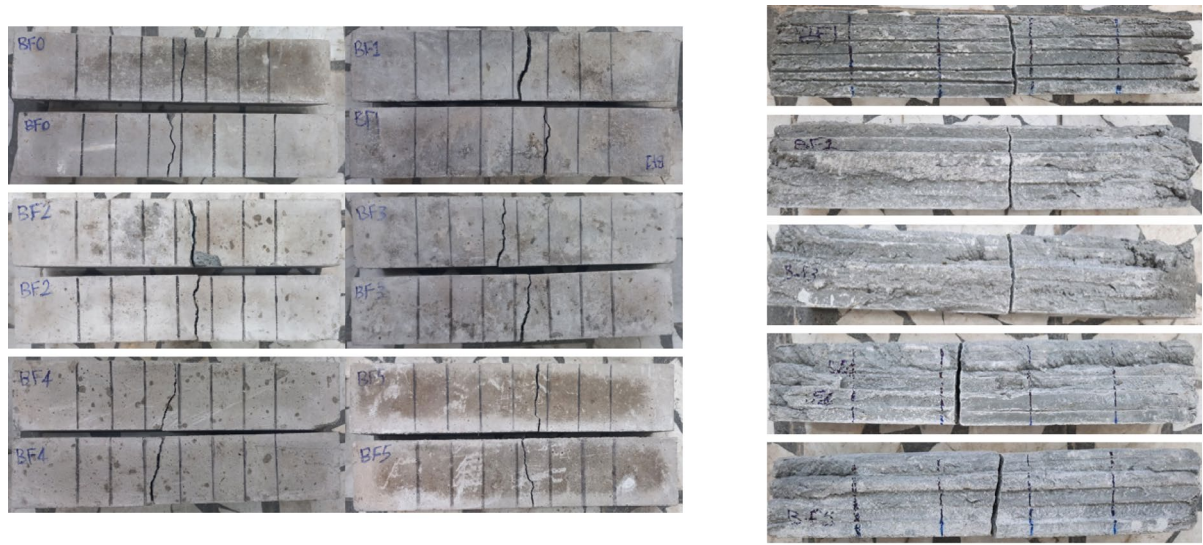


Fig. 22. Typical failure pattern of flexural specimens.

- Adding natural fibers in the mixture can reduce the resting time of the extruded filaments. All the mixtures had problems to be extruded after 60 min and the extruded length decreased after 30 min. In the mixture without fibers, the extruded length was “15 cm” in 60 min, and this length reached “10 cm” for the mixture containing 0.2% of fibers.
- The addition of 0.1, 0.15, and 0.2% fibers improved the compressive strength by 20, 26, and 28%, respectively. However, adding more fibers to the mixture (0.25% vol) did not significantly increase the compressive strength, and less than 0.2% of the fibers were observed in most of the mixtures. Also, the compressive strength of the printed samples in all three loading directions was lower than that of the cast samples.
- Using natural fibers increases the tensile strength so that the mixtures containing 0.1% fibers up to 46% and 0.2% fibers up to 66% improvement in tensile strength. For mixtures containing DPF and BF, the addition of 0.25% fibers did not have a significant increase in tensile strength. Adding 0.2% fibers for these mixtures had the best results in the direct tensile test.
- Adding natural fibers to the mixture up to 0.25% compared to the mix without fibers improved the flexural strength. Similar to the samples with the mold, increasing the amount of fibers leads to an increase in the final bending force in the printed samples. Printed beams with 0.2% fibers showed higher ductility and energy absorption than cast specimens, particularly in the Z direction, highlighting the potential for structural applications.

A comparative analysis of the natural fibers used in this study reveals that date palm and coconut fibers at a 0.2% volume fraction provided the best balance of printability and mechanical performance compared to cob skin, banana, and pineapple leaf fibers. Specifically, date palm fibers achieved a 25% higher flexural strength in the Z direction and a 28% increase in compressive strength compared to the control mix, attributed to their smaller diameter and enhanced fiber-matrix bonding. Coconut fibers similarly improved extrudability and buildability, with extruded filament lengths up to 300 mm, outperforming banana and cob skin fibers, which exhibited reduced flowability and extrudability due to larger diameters. These findings align with prior research indicating that natural fibers with high cellulose content and optimal morphology enhance 3D-printed concrete's performance.

Potential applications include sustainable precast elements, architectural facades, and lightweight structural components, leveraging the environmental benefits of bio-waste fibers. Future research should explore hybrid fiber systems, long-term durability, and scalability to advance the adoption of natural fiber-reinforced 3DCP in construction.

Tests	F1-0.1DPF	F2-0.1CF	F3-0.1BF	F4-0.1PALF	F5-0.1Coir	F6-0.25DPF	F7-0.25CF	F8-0.25BF	F9-0.25PALF	F10-0.25Coir	F11-0.15DPF	F12-0.15CF	F13-0.15BF	F14-0.15PALF	F15-0.15Coir	F16-0.2DPF	F17-0.2CF	F18-0.2BF	F19-0.2PALF	F20-0.2Coir
Fresh Properties	Flowability	×	×	×							×	×								
	Extrudability										×	×				×	×	×		
	Printability										×	×								
	Buildability					×														x
Hardened Properties	Open time	×	×	×																
	Compressive Strength (24 h)															×	×			x
	Tensile Strength (28 days)										×	×					×			
	Flexural Strength (28 days)																			x

Table 4. Optimum 3D printable mix design based on experimental results conducted in the present study.

Data availability

Some or all data, models, or code that support the findings of this study are available from the corresponding author upon reasonable request.

Received: 5 March 2025; Accepted: 25 September 2025

Published online: 31 October 2025

References

1. Testing, A. S. .f. and M.C.C.-o. (ed Cement) Standard Test Method for Compressive Strength of Hydraulic Cement Mortars (Using 2-in. Or [50-mm] Cube Specimens). ASTM Standards 4.1: 1-9.
2. Tay, Y. W. D. et al. 3D printing trends in Building and construction industry: a review. *Virtual Phys. Prototyp.* **12** (3), 261–276 (2017).
3. Buswell, R. A. et al. 3D printing using concrete extrusion: A roadmap for research. *Cem. Concr. Res.* **112**, 37–49 (2018).
4. Zhang, J. et al. A review of the current progress and application of 3D printed concrete. *Compos. Part A: Appl. Sci. Manufac.* **125**, 105533 (2019).
5. Sonebi, M. et al. *Effect of red Mud, Nanoclay, and natural fiber on fresh and rheological properties of Three-Dimensional concrete printing*. *ACI Mater. J.*, **118**(6), 97–110 (2021).
6. Roussel, N. Rheological requirements for printable concretes. *Cem. Concr. Res.* **112**, 76–85 (2018).
7. Wolfs, R., Bos, F. & Salet, T. Hardened properties of 3D printed concrete: the influence of process parameters on interlayer adhesion. *Cem. Concr. Res.* **119**, 132–140 (2019).
8. Liu, X. et al. Study on the properties of an ecotype mortar with rice husks and Sisal fibers. *Adv. Civil Eng.* **2021** (1), 5513303 (2021).
9. Luhar, S. et al. Sustainable and renewable bio-based natural fibres and its application for 3D printed concrete: A review. *Sustainability* **12** (24), 10485 (2020).
10. Perrot, A., Rangeard, D. & Pierre, A. Structural built-up of cement-based materials used for 3D-printing extrusion techniques. *Mater. Struct.* **49**, 1213–1220 (2016).
11. Panda, B. & Tan, M. J. Experimental study on mix proportion and fresh properties of fly Ash based geopolymer for 3D concrete printing. *Ceram. Int.* **44** (9), 10258–10265 (2018).
12. Tang, Z. et al. Biomodification of bond performance of coconut fiber in cement mortar to enhance damping behavior. *J. Mater. Civ. Eng.* **35** (10), 04023351 (2023).
13. Momoh, E. O., Osoforo, A. I. & Menshykov, O. Physicomechanical properties of treated oil palm-broom fibers for cementitious composites. *J. Mater. Civ. Eng.* **32** (10), 04020300 (2020).
14. Wei, J. & Genceturk, B. Degradation of natural fiber in cement composites containing diatomaceous Earth. *J. Mater. Civ. Eng.* **30** (11), 04018282 (2018).
15. Kornienko, K. & Łach, M. Geopolymers reinforced by short and long fibres—innovative materials for additive manufacturing. *Curr. Opin. Chem. Eng.* **28**, 167–172 (2020).
16. Panda, B., Paul, S. C. & Tan, M. J. Anisotropic mechanical performance of 3D printed fiber reinforced sustainable construction material. *Mater. Lett.* **209**, 146–149 (2017).
17. Nematollahi, B. et al. Effect of polypropylene fibre addition on properties of geopolymers made by 3D printing for digital construction. *Materials* **11** (12), 2352 (2018).
18. Nematollahi, B. et al. Effect of type of fiber on inter-layer bond and flexural strengths of extrusion-based 3D printed geopolymer, *Mater. Sci. Forum*, 939 (2018) 155–193516.1936
19. Ali, M. et al. Mechanical and dynamic properties of coconut fibre reinforced concrete. *Constr. Build. Mater.* **30**, 814–825 (2012).
20. Pickering, K. L., Efendi, M. A. & Le, T. M. A review of recent developments in natural fibre composites and their mechanical performance. *Compos. Part A: Appl. Sci. Manufac.* **83**, 98–112 (2016).
21. El-Sabbagh, A. Effect of coupling agent on natural fibre in natural fibre/polypropylene composites on mechanical and thermal behaviour. *Compos. Part. B: Eng.* **57**, 126–135 (2014).
22. Al-Maharma, A. Y., Patil, S. P. & Markert, B. *Environmental Impact Analysis of Plant Fibers and their Composites Relative To their Synthetic Counterparts Based on Life Cycle Assessment approach*, in *Advances in bio-based Fiberp*. 741–781 (Elsevier, 2022).
23. Silva, G. et al. Development of a stabilized natural fiber-reinforced earth composite for construction applications using 3D printing. in *IOP Conference Series: Materials Science and Engineering*. IOP Publishing. (2019).
24. Mousavi, S. & Dehestani, M. Influence of latex and vinyl disposable gloves as recycled fibers in 3D printing sustainable mortars. *Sustainability* **14** (16), 9908 (2022).
25. Tan, K. Predicting compressive strength of recycled concrete for construction 3D printing based on statistical analysis of various neural networks. *J. Building Constr. Plann. Res.* **6** (02), 71 (2018).
26. Lu, Y., Xiao, J. & Li, Y. 3D printing recycled concrete incorporating plant fibres: A comprehensive review. *Constr. Build. Mater.* **425**, 135951 (2024).
27. Chen, Y. et al. The effect of viscosity-modifying admixture on the extrudability of limestone and calcined clay-based cementitious material for extrusion-based 3D concrete printing. *Materials* **12** (9), 1374 (2019).
28. Marchon, D. et al. Hydration and rheology control of concrete for digital fabrication: potential admixtures and cement chemistry. *Cem. Concr. Res.* **112**, 96–110 (2018).
29. Salman, N. M. et al. Importance and potential of cellulosic materials and derivatives in extrusion-based 3D concrete printing (3DCP): prospects and challenges. *Constr. Build. Mater.* **291**, 123281 (2021).
30. Carcassi, O. B. et al. Maximizing fiber content in 3D-printed Earth materials: Printability, mechanical, thermal and environmental assessments. *Constr. Build. Mater.* **425**, 135891 (2024).
31. Onuaguluchi, O. & Banthia, N. Plant-based natural fibre reinforced cement composites: A review. *Cem. Concr. Compos.* **68**, 96–108 (2016).
32. Dey, D. et al. Use of industrial waste materials for 3D printing of sustainable concrete: A review. *J. Clean. Prod.* **340**, 130749 (2022).
33. Tu, H. et al. Recent advancements and future trends in 3D concrete printing using waste materials. *Developments Built Environ.* **16**, 100187 (2023).
34. Bai, G. et al. 3D printing eco-friendly concrete containing under-utilised and waste solids as aggregates. *Cem. Concr. Compos.* **120**, 104037 (2021).
35. Pasupathy, K., Ramakrishnan, S. & Sanjayan, J. 3D concrete printing of eco-friendly geopolymer containing brick waste. *Cem. Concr. Compos.* **138**, 104943 (2023).
36. Mousavi, S. S. & Dehestani, M. Influence of latex and vinyl disposable gloves as recycled fibers in 3D printing sustainable mortars. *Sustainability* **14** (16), 9908 (2022).
37. Ding, T. et al. Anisotropic behavior in bending of 3D printed concrete reinforced with fibers. *Compos. Struct.* **254**, 112808 (2020).
38. Li, H. et al. Methodology to design eco-friendly fiber-reinforced concrete for 3D printing. *Cem. Concr. Compos.* **147**, 105415 (2024).
39. Tran, M. V., Cu, Y. T. & Le, C. V. Rheology and shrinkage of concrete using polypropylene fiber for 3D concrete printing. *J. Building Eng.* **44**, 103400 (2021).

40. Mousavi, S. S. & Dehestani, M. On the possibility of using waste disposable gloves as recycled fibers in sustainable 3D concrete printing using different additives. *Sci. Rep.* **13** (1), 10812 (2023).
41. ASTM, C. *Standard test method for sieve analysis of fine and coarse aggregates. ASTM C136-06*, (2006).
42. Rihayat, T. et al. *Synthesis and characterization of PLA-Chitosan-ZnO composite for packaging biofilms*. in *IOP Conference Series: Materials Science and Engineering*. IOP Publishing. (2020).
43. Lv, C. et al. Properties of 3D printing fiber-reinforced geopolymers based on interlayer bonding and anisotropy. *Materials* **15** (22), 8032 (2022).
44. Abdellah, M. Y. et al. Characteristic properties of date-palm fibre/sheep wool reinforced polyester composites. *J. Bioresources Bioprod.* **8** (4), 430–443 (2023).
45. Oushabi, A. et al. The effect of alkali treatment on mechanical, morphological and thermal properties of date palm fibers (DPFs): study of the interface of DPF-Polyurethane composite. *S. Afr. J. Chem. Eng.* **23**, 116–123 (2017).
46. Montreuil, A. et al. Flax fiber treatment by an alkali solution and Poly (dopamine) coating: effects on the fiber physico-chemistry and flax/Elium® composite interfacial properties. *Compos. Part A: Appl. Sci. Manufac.* **177**, 107963 (2024).
47. Nurazzi, N. et al. Thermogravimetric analysis properties of cellulosic natural fiber polymer composites: A review on influence of chemical treatments. *Polymers* **13** (16), 2710 (2021).
48. ASTM, C. *305, Standard Practice for Mechanical Mixing of Hydraulic Cement Pastes and Mortars of Plastic Consistency* (ASTM International, 1999).
49. International, A. *ASTM C1437-15 Standard Test Method for Flow of Hydraulic Cement Mortar* (ASTM International West Conshohocken, 2015).
50. Ma, G., Li, Z. & Wang, L. Printable properties of cementitious material containing copper tailings for extrusion based 3D printing. *Constr. Build. Mater.* **162**, 613–627 (2018).
51. Arunothayan, A. R. et al. Development of 3D-printable ultra-high performance fiber-reinforced concrete for digital construction. *Constr. Build. Mater.* **257**, 119546 (2020).
52. Ivanova, I. et al. Comparison between methods for indirect assessment of buildability in fresh 3D printed mortar and concrete. *Cem. Concr. Res.* **156**, 106764 (2022).
53. Wolfs, R., Bos, F. & Salet, T. Triaxial compression testing on early age concrete for numerical analysis of 3D concrete printing. *Cem. Concr. Compos.* **104**, 103344 (2019).
54. ASTM. *ASTM C109: Standard test method for compressive strength of hydraulic cement mortars (Using 2-in. or [50-mm] cube specimens)*. (2005).
55. Pi, Z. et al. Effects of brass coating and nano-SiO₂ coating on steel fiber–matrix interfacial properties of cement-based composite. *Compos. Part. B: Eng.* **189**, 107904 (2020).
56. Mohammed, A. A. & Mohammed, I. I. Effect of fiber parameters on the strength properties of concrete reinforced with PET waste fibers. *Iran. J. Sci. Technol. Trans. Civil Eng.* **45** (3), 1493–1509 (2021).
57. Pi, Z. et al. Interfacial microstructure and bond strength of nano-SiO₂-coated steel fibers in cement matrix. *Cem. Concr. Compos.* **103**, 1–10 (2019).
58. Esmaili, J. et al. Pull-out and bond-slip performance of steel fibers with various ends shapes embedded in polymer-modified concrete. *Constr. Build. Mater.* **271**, 121531 (2021).
59. Monazami, M. & Gupta, R. Effect of curing age on pull-out response of carbon, steel, and synthetic fiber embedded in cementitious mortar matrix. *J. Mater. Civ. Eng.* **34** (10), 04022275 (2022).
60. Madueke, C. I., Mbah, O. M. & Umunakwe, R. A review on the limitations of natural fibres and natural fibre composites with emphasis on tensile strength using Coir as a case study. *Polym. Bull.* **80** (4), 3489–3506 (2023).
61. Virk, A. S., Hall, W. & Summerscales, J. Modulus and strength prediction for natural fibre composites. *Mater. Sci. Technol.* **28** (7), 864–871 (2012).
62. Wu, Z., Khayat, K. H. & Shi, C. Effect of nano-SiO₂ particles and curing time on development of fiber-matrix bond properties and microstructure of ultra-high strength concrete. *Cem. Concr. Res.* **95**, 247–256 (2017).
63. Boshoff, W. P., Mechtcherine, V. & van Zijl, G. P. Characterising the time-dependant behaviour on the single fibre level of SHCC: part 2: the rate effects on fibre pull-out tests. *Cem. Concr. Res.* **39** (9), 787–797 (2009).
64. Xu, M., Hallinan, B. & Wille, K. Effect of loading rates on pullout behavior of high strength steel fibers embedded in ultra-high performance concrete. *Cem. Concr. Compos.* **70**, 98–109 (2016).
65. Chen, Y. et al. 3D printing of calcined clay-limestone-based cementitious materials. *Cem. Concr. Res.* **149**, 106553 (2021).
66. Şahin, H. G., Akgümüş, F. E. & Mardani, A. *Mechanical and Rheological Properties of Fiber-reinforced 3D Printable concrete; in Terms of Fiber Content and Aspect Ratio* (Structural Concrete, 2024).
67. Şahin, H. G., Mardani, A. & Beytekin, H. E. Effect of silica fume utilization on structural build-up, mechanical and dimensional stability performance of fiber-reinforced 3D printable concrete. *Polymers* **16** (4), 556 (2024).
68. Rahul, A. et al. 3D printable concrete: mixture design and test methods. *Cem. Concr. Compos.* **97**, 13–23 (2019).
69. Nerella, V. et al. Inline quantification of extrudability of cementitious materials for digital construction. *Cem. Concr. Compos.* **95**, 260–270 (2019).
70. Kaliyavaradhan, S. K. et al. Effect of sand gradations on the fresh properties of 3D printable concrete. *Magazine Concrete Res.* **76** (16), 903–912 (2024).
71. Panda, B. et al. Additive manufacturing of geopolymer for sustainable built environment. *J. Clean. Prod.* **167**, 281–288 (2017).
72. Özalp, F. & Yilmaz, H. D. Fresh and hardened properties of 3D high-strength printing concrete and its recent applications. *Iran. J. Sci. Technol. Trans. Civil Eng.* **44** (Suppl 1), 319–330 (2020).
73. Zhang, Y. et al. Rheological and Harden properties of the high-thixotropy 3D printing concrete. *Constr. Build. Mater.* **201**, 278–285 (2019).
74. Ta, M. P. B. et al. *The effect of printing direction on strength of 3D printed concrete*. JOURNAL OF MATERIALS & CONSTRUCTION, 12(02). (2022).
75. Hambach, M., Rutzen, M. & Volkmer, D. *Properties of 3D-printed fiber-reinforced Portland Cement paste, in 3D Concrete Printing Technologyp*. 73–113 (Elsevier, 2019).
76. Rihayat, T. et al. *Green composites of natural fiber bamboo/pineapple leaf/coconut husk as hybrid materials*. in *IOP Conference Series: Materials Science and Engineering*. IOP Publishing. (2020).
77. Testing, A. S. M.C.C.-o. Concrete, and C. Aggregates, *Standard test method for flexural performance of fiber-reinforced concrete (using beam with third-point loading)*. : ASTM International. (2013).
78. Nwankwo, C. O. & Ede, A. N. Flexural strengthening of reinforced concrete beam using a natural fibre reinforced polymer laminate: an experimental and numerical study. *Mater. Struct.* **53** (6), 142 (2020).
79. Rescalvo, F. J. et al. Experimental and analytical analysis for bending load capacity of old timber beams with defects when reinforced with carbon fiber strips. *Compos. Struct.* **186**, 29–38 (2018).
80. Ebrahim, A. et al. *Enhancing polymer composites with date palm residues for sustainable innovation: a review*. *Int. J. Mater. Res.*, **116**(4), 225–239 (2025).
81. Mittal, M. & Chaudhary, R. Experimental study on the water absorption and surface characteristics of alkali treated pineapple leaf fibre and coconut husk fibre. *Int. J. Appl. Eng. Res.* **13** (15), 12237–12243 (2018).
82. Pothan, L. A. & Thomas, S. Effect of hybridization and chemical modification on the water-absorption behavior of banana fiber-reinforced polyester composites. *J. Appl. Polym. Sci.* **91** (6), 3856–3865 (2004).

83. Rinawa, M. L. et al. Water absorption studies of pineapple leaf fiber/nano rice husk powder reinforced epoxy matrix hybrid composites. *Mater. Today: Proc.* **59**, 1498–1502 (2022).
84. Tran, L. Q. N. et al. Understanding the interfacial compatibility and adhesion of natural Coir fibre thermoplastic composites. *Compos. Sci. Technol.* **80**, 23–30 (2013).

Acknowledgements

The authors would like to thank the concrete and structural laboratories of Babol Noshirvani University of Technology in Iran for their support in our experiments.

Author contributions

CRediT authorship contribution statement Sajad Garshasbi: Conceptualization, Methodology, Investigation, Visualization, Validation, Formal analysis, Writing – original draft, Writing – review & editing. Seyed Sina Mousavi: Conceptualization, Methodology, Data Curation, Formal analysis, Validation, Writing – original draft, Writing – review & editing. Mehdi Dehestani: Conceptualization, Methodology, Supervision, Project administration, Data curation, Validation, Writing – review & editing. Hadi Nazarpour: Supervision, Data curation, Project administration.

Declarations

Competing interests

The authors declare no competing interests.

Additional information

Correspondence and requests for materials should be addressed to M.D.

Reprints and permissions information is available at www.nature.com/reprints.

Publisher's note Springer Nature remains neutral with regard to jurisdictional claims in published maps and institutional affiliations.

Open Access This article is licensed under a Creative Commons Attribution-NonCommercial-NoDerivatives 4.0 International License, which permits any non-commercial use, sharing, distribution and reproduction in any medium or format, as long as you give appropriate credit to the original author(s) and the source, provide a link to the Creative Commons licence, and indicate if you modified the licensed material. You do not have permission under this licence to share adapted material derived from this article or parts of it. The images or other third party material in this article are included in the article's Creative Commons licence, unless indicated otherwise in a credit line to the material. If material is not included in the article's Creative Commons licence and your intended use is not permitted by statutory regulation or exceeds the permitted use, you will need to obtain permission directly from the copyright holder. To view a copy of this licence, visit <http://creativecommons.org/licenses/by-nc-nd/4.0/>.

© The Author(s) 2025